European Journal of Medicinal Chemistry 203 (2020) 112618

Contents lists available at ScienceDirect

European Journal of Medicinal Chemistry

journal homepage: http://www.elsevier.com/locate/ejmech

Research paper

Discovery of tertiary amide derivatives incorporating benzothiazole moiety as anti-gastric cancer agents *in vitro* via inhibiting tubulin polymerization and activating the Hippo signaling pathway

Jian Song [a, b, 1], Qiu-Lei Gao [a, b, e, 1], Bo-Wen Wu [a, b], Ting Zhu [a, b], Xin-Xin Cui [a, b], Cheng-Jun Jin [a, b], Shu-Yu Wang [a, b], Sheng-Hui Wang [a, b], Dong-Jun Fu [d], Hong-Min Liu [a, b], Sai-Yang Zhang [a, b, c, *], Yan-Bing Zhang [a, b, **], Yong-Chun Li [a, b, ***]

[a] *Institute of Drug Discovery & Development, School of Basic Medical Sciences, Zhengzhou University, Zhengzhou, 450001, China*
[b] *School of Pharmaceutical Sciences, Key Laboratory of Advanced Drug Preparation Technologies (Ministry of Education), Zhengzhou University, Zhengzhou, 450001, China*
[c] *Henan Institute of Advanced Technology, Zhengzhou University, Zhengzhou, 450001, China*
[d] *Modern Research Center for Traditional Chinese Medicine, School of Chinese Materia Medica, Beijing University of Chinese Medicine, Beijing, 100029, China*
[e] *School of Mechanics and Safety Engineering, ZhengZhou University, China*

ARTICLE INFO

Article history:
Received 27 April 2020
Received in revised form
23 June 2020
Accepted 23 June 2020
Available online 13 July 2020

Keywords:
Gastric cancer
Tertiary amide
Benzothiazole
Colchicine binding site tubulin inhibitor
Hippo signaling pathway

ABSTRACT

On the basis and continuation of our previous studies on anti-tubulin and anti-gastric cancer agents, novel tertiary amide derivatives incorporating benzothiazole moiety were synthesized and the anti-proliferative activity was studied *in vitro*. Preliminary structure activity relationships (SARs) were explored according to the *in vitro* antiproliferative activity results. Some of compounds could significantly inhibit the proliferation of three cancer cells (HCT-116, MGC-803 and PC-3 cells) and compound **F10** exhibited excellent antiproliferative activity against HCT-116 cells (IC_{50} = 0.182 μM), MGC-803 cells (IC_{50} = 0.035 μM), PC-3 cells(IC_{50} = 2.11 μM) and SGC-7901 cells (IC_{50} = 0.049 μM). Compound **F10** effectively inhibited tubulin polymerization (IC_{50} = 1.9 μM) and bound to colchicine binding site of tubulin. Molecular docking results suggested compound **F10** could bind tightly into the colchicine binding site of β-tubulin. Moreover, compound **F10** could regulate the Hippo/YAP signaling pathway. Compound **F10** activated Hippo signaling pathway from its very beginning MST1/2, as the result of Hippo cascade activation YAP were inhibited. And then it led to a decrease of c-Myc and Bcl-2 expression. Further molecular experiments showed that compound **F10** arrested at G2/M phase, inhibited cell colony formatting and induced extrinsic and intrinsic apoptosis in MGC-803 and SGC-7901 cells. Collectively, compound **F10** was the first to be reported as a new anticancer agent *in vitro* via inhibiting tubulin polymerization and activating the Hippo signaling pathway.

1. Introduction

Gastric cancer (GC) is one of the most aggressive and common cancers in the world. In 2018, there were over 1000000 new cases diagnosed worldwide and an estimated 783,000 people died of gastric cancer [1]. Although cancer diagnosis technology and anti-cancer agents have been evolving steadily, gastric cancer remains one of the most lethal malignant tumors among China [2–4]. Therefore, it is urgent to develop novel agents for the treatment of gastric cancer.

Microtubule (composed of α-tubulin and β-tubulin heterodimers)

* Corresponding author. Henan Institute of Advanced Technology, Zhengzhou University, Zhengzhou 450001, China.
** Corresponding author. School of Pharmaceutical Sciences, Key Laboratory of Advanced Drug Preparation Technologies (Ministry of Education), Zhengzhou University, Zhengzhou 450001, China.
*** Corresponding author. Institute of Drug Discovery & Development, School of Basic Medical Sciences, Zhengzhou University, Zhengzhou 450001, China.
E-mail addresses: saiyangz@zzu.edu.cn (S.-Y. Zhang), zhangyb@zzu.edu.cn (Y.-B. Zhang), ycli78@zzu.edu.cn (Y.-C. Li).
[1] These authors contributed equally to this work.

https://doi.org/10.1016/j.ejmech.2020.112618
0223-5234/

is a component of the cytoskeleton and plays an important role in cellular shape maintenance, mitosis, signal transduction and material transportation [5–7]. Because of its significant role in the mitosis and growth of eukaryotic cells, microtubule system has been regarded as an attractive and successful molecular target for the treatment of cancers as chemotherapeutic agents [8–13] such as paclitaxel [11], vincristine [12] and vinblastine [13]. But the marketed tubulin inhibitors used in clinical treatment (e.g. paclitaxel/taxol, vincristine, vinblastine) bind to the taxanes or vinca alkaloids binding sites in tubulin [14,15]. Unfortunately, they general have poor in water solubility, toxic, side effects, and drug resistance [10,16,17]. Therefore, polymerization inhibitors targeting tubulin colchicine binding site have received extraordinary attention in the recent years, importantly tubulin inhibitors targeting colchicine binding site could largely overcome the above drawbacks and have more therapeutic advantages over other binding sites tubulin inhibitors [18–21].

To date, various tubulin inhibitors that target colchicine binding site have been developed [22–27] and some of them have entered clinical trials [28–32] such as **CA-4P** [29], **ZD6126** [30] and **ABT-751** [31]. In addition, our group have reported several series colchicine binding site anti-tubulin agents against gastric cancers [33–35]. For example, β-lactam-azide analogue **1** played excellent anticancer activity against MGC-803 cells ($IC_{50} = 0.106$ μM) and was identified as colchicine binding site tubulin inhibitor ($IC_{50} = 2.26$ μM)[31]. What's more, benzothiazole moiety has been reported as a potential antitumor fragment to design colchicine binding site tubulin inhibitors [36–38] such as compound **2** [38] and **3** [36]with IC_{50} values of 1.67 μM and 2.01 μM, respectively (Fig. 1).

Hippo is a highly conserved signaling pathway which plays an crucial role in the occurrence and growth of most tumors by regulating cell proliferation and apoptosis [39–41]. The activation of Hippo signaling pathway can affect the genesis, proliferation, drug resistance and metastasis of tumor stem cells [42]. In mammals, Hippo signaling pathway consists of protein kinases MST1/2, SAV1, LATS1/2, MOB1, and downstream effectors YAP, TAZ and TEADs. Activated YAP and TEADs together express oncogenes like c-Myc and Bcl-2 and would contribute to the development of tumors, such as colorectal cancer [42], lung cancer [43], breast cancer [44], gastric cancer [45]. What's more, it also has been found to functionally interact with many other cellular pathways and act as a central node in the regulation of cell division in various cancers including gastric cancer [46–48]. Activation of Hippo pathway would result in phosphorylation of YAP. The phosphor-YAP is inactivated and would be degraded via Ubiquitin-proteasome system. Herein, targeting the Hippo pathway with small molecule inhibitors may represent a potential approach to treat cancers with high YAP activity. However, only rare small molecule activators of Hippo pathway have been reported.

In this work, as the continuation of our studies on colchicine binding site tubulin inhibitors and anti-gastric cancer agents, novel tertiary amide derivatives incorporating benzothiazole moiety were designed via opening ring of β-lactam and explored its antiproliferative activity (Fig. 2). We screened the most potent antiproliferative activity compound **F10** through *in vitro* tubulin polymerization assay and Hippo related protein expression in MGC-803 and SGC-7901 cells. Fortunately, compound **F10** is a novel colchicine binding site tubulin inhibitor and could activate the Hippo signaling pathway. Therefore, we first report novel tertiary amide derivatives incorporating benzothiazole moiety as new anti-gastric cancer agents *in vitro* via inhibiting tubulin polymerization and activating the Hippo signaling pathway.

2. Chemistry

The chemical synthesis of compounds incorporating benzothiazole moiety is outlined in Scheme 1. Substituted benzaldehyde derivatives **A1-A10** reacted with 3,4,5-trimethoxyaniline (**B**) to afford compounds **C1-C10** in EtOH. Compounds **C1-C10** then reacted with $NaBH_4$ in the presence of benzoic acid in DCM to give compounds **D1-D10**. Then compounds **D1-D10** reacted with chloroacetyl chloride to give compounds **E1-E11** in DMF. Finally, compounds **E1-E11** was reacted with substituted benzothiazoles to afford the target compounds **F1-F14** in the presence of K_2CO_3 in acetonitrile. Furthermore, compound **B** reacted with substituted benzyl chlorides **G1-G6** to afford compounds **H1-H6** in the presence of K_2CO_3 in DMF. Next, compounds **H1-H6** reacted with

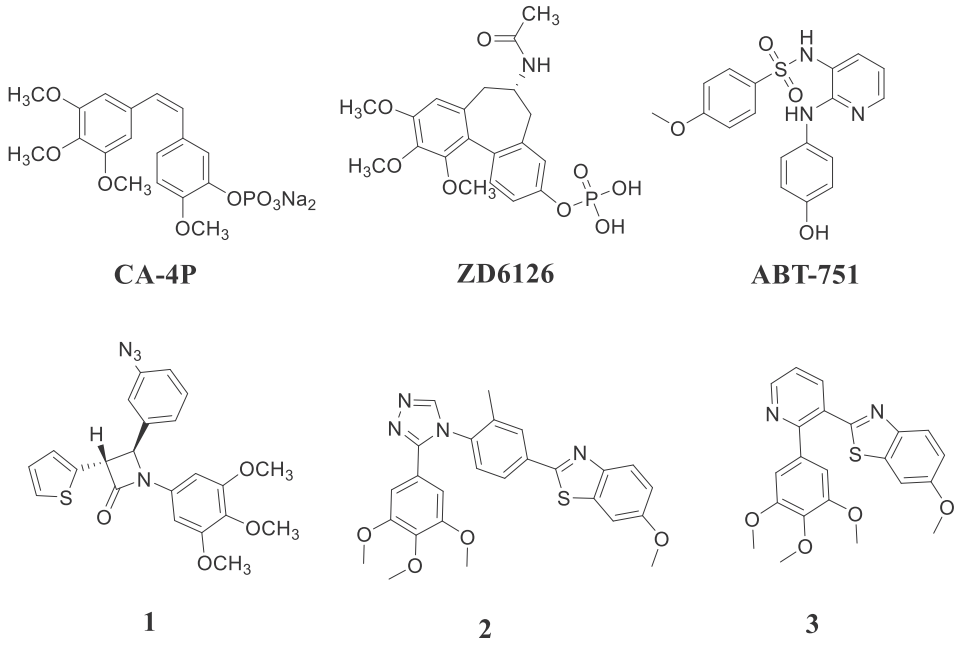

Fig. 1. Structures of colchicine binding site tubulin inhibitors.

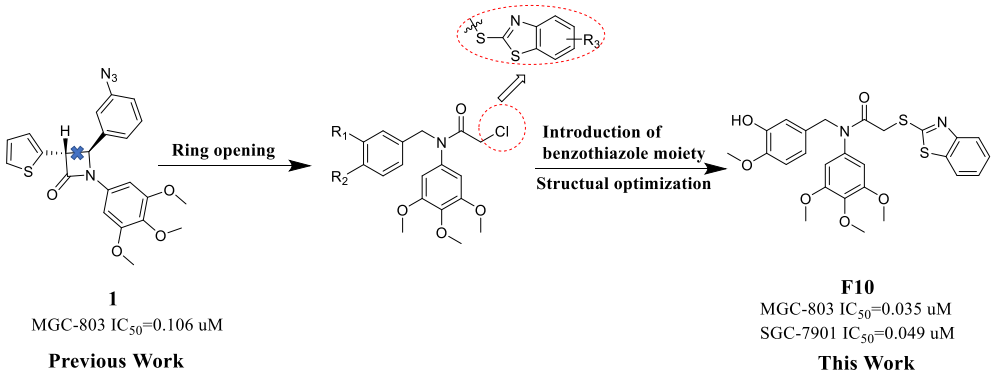

Fig. 2. Design of tertiary amide derivative F10 in this work.

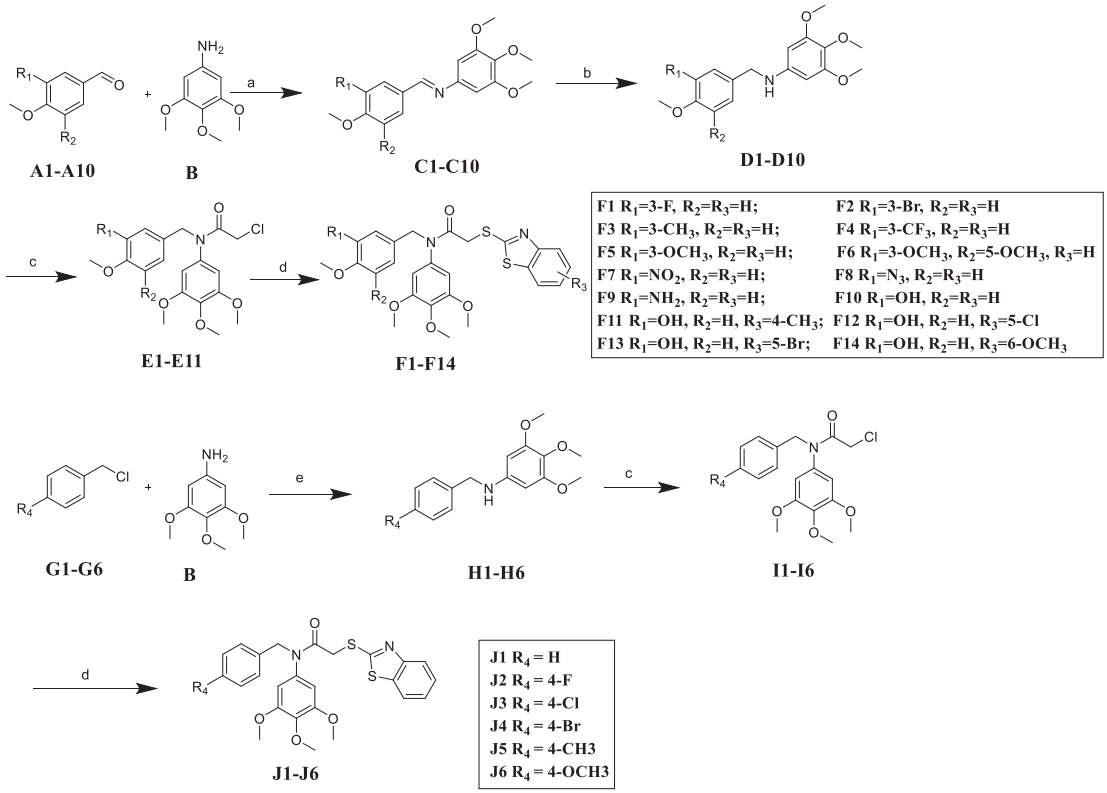

Scheme 1. Synthesis of target compounds **F1-F14** and **J1-J6**. Reagents and conditions: a) EtOH, 80 °C, 6 h; b) Benzoic acid, $NaBH_4$, anhydrous CH_2Cl_2, rt, 8 h; c) chloroacetyl chloride, DMF, rt. d) substituted benzothiazoles, acetonitrile, K_2CO_3, reflux, 6 h; e) substituted benzyl chlorides, DMF, K_2CO_3, rt, 7 h.

chloroacetyl chloride in DMF to obtain tertiary amide derivatives **I1-I6**. Tertiary amide derivatives **I1-I6** then reacted with 2-mercaptobenzothiazole in the presence of K_2CO_3 in acetonitrile to afford the target compounds **J1-J6.** Characterization of compounds **F1-F14** and **J1-J6** was carried out by means of NMR and HREI-mass spectra.

3. Results and discussion

3.1. Antiproliferative activity and structure activity relationships

The antiproliferative activity of synthesized compounds **F1-F14** and **J1-J6** was evaluated against MGC-803 cell line (human gastric cancer), HCT-116 cell line (human colon cancer) and PC-3 cell line (human prostate cancer) using MTT assay and 5-fluorouracil and colchicine as control drugs. The antiproliferative activity results are depicted in https://www.sciencedirect.com/science/article/pii/S0223523419306440 - tbl1 Table 1 and https://www.sciencedirect.com/science/article/pii/S0223523419306440 - tbl2 Table 2. The structure-activity relationships of synthesized compounds **F1-F14** and **J1-J6** are preliminarily summarized (Fig. 3).

The *in vitro* antiproliferative efficacy of compounds **F1-F14** are listed in Table 1. In this series of compounds, we primarily explored the importance of the substituent groups on phenyl ring (A ring) and benzothiazole moiety (B ring) in antiproliferative activity. As shown in https://www.sciencedirect.com/science/article/pii/S0223523418309280 - tbl1 Table 1, most of synthetic compounds displayed moderate to excellent antiproliferative activity. The *in vitro* antiproliferative efficacy of the compounds varies with its substituent groups on the ring A. Compounds **F1-F2** and **F7-F14** inhibited MGC-803 cells growth

Table 1
Antiproliferative activity of compounds **F1**-**F14** against MGC-803, HCT-116 and PC-3 cells.

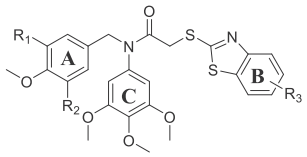

Compound	R_1	R_2	R_3	IC_{50} (μmol/L)[a]		
				MGC-803	HCT-116	PC-3
F1	-F	H	H	0.416 ± 0.021	1.83 ± 0.26	20.1 ± 2.02
F2	-Br	H	H	0.852 ± 0.72	4.55 ± 1.35	16.0 ± 1.38
F3	$-CH_3$	H	H	6.36 ± 0.89	17.1 ± 2.42	34.3 ± 2.04
F4	$-CF_3$	H	H	25.2 ± 1.64	>80	>80
F5	$-OCH_3$	H	H	34.1 ± 2.13	33.9 ± 2.49	>80
F6	$-OCH_3$	$-OCH_3$	H	45.7 ± 1.83	65.3 ± 2.54	>80
F7	NO_2	H	H	0.682 ± 0.052	1.28 ± 0.11	26.5 ± 2.68
F8	$-N_3$	H	H	0.187 ± 0.027	2.86 ± 1.69	14.4 ± 1.72
F9	$-NH_2$	H	H	0.084 ± 0.017	0.491 ± 0.025	7.51 ± 2.58
F10	-OH	H	H	**0.035 ± 0.006**	**0.182 ± 0.012**	**2.11 ± 0.76**
F11	-OH	H	$4-CH_3$	0.493 ± 0.033	0.852 ± 0.098	12.3 ± 1.84
F12	-OH	H	5-Cl	0.085 ± 0.012	0.429 ± 0.063	11.2 ± 1.65
F13	-OH	H	5-Br	0.372 ± 0.028	3.38 ± 1.25	8.21 ± 1.18
F14	-OH	H	$6-OCH_3$	0.071 ± 0.009	0.352 ± 0.043	4.11 ± 0.84
5-FU	–	–	–	6.82 ± 1.17	13.8 ± 1.96	18.4 ± 1.73
Colchicine	–	–	–	0.107 ± 0.010	0.129 ± 0.020	0.338 ± 0.014
CA-4P	–	–	–	0.020 ± 0.002	0.042 ± 0.006	0.033 ± 0.004

[a] Antiproliferative activity was assayed by exposure for 48 h.

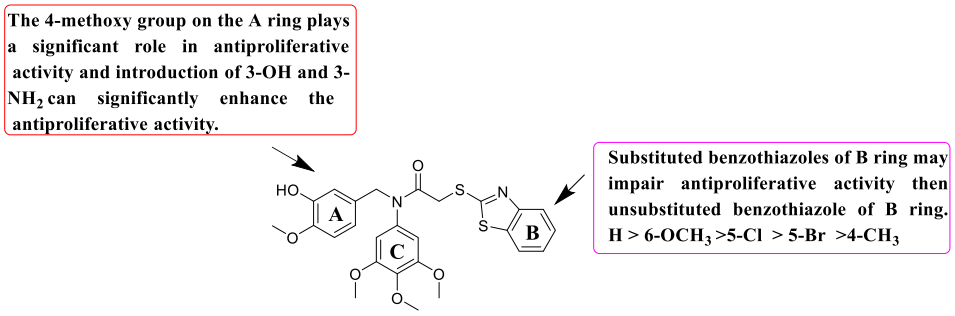

Fig. 3. Summary of the structure-activity relationships.

with IC_{50} values less than 1 μM and inhibited the growth of HCT-116 cells with IC_{50} values less than 5 μM. But most of compounds exhibited weaker antiproliferative activity against PC-3 cells compared to MGC-803 cells and HCT-116 cells. Only compounds **F9**, **F10** and **F13** showed the potent antiproliferative activity of PC-3 cells with IC_{50} values less than 10 μM. To our delight, compound **F10** with 3-hydroxyl group and 4-methoxy group on the ring A exhibited most active activity with IC_{50} values of 0.035 μM (MGC-803 cells), 0.182 μM (HCT-116 cells) and 2.11 μM (PC-3 cells). Compounds **F1**, **F2**, **F4** and **F7** showed improved efficacy against MGC-803 cells with electron-withdrawing groups on the ring A compared to compounds **F3**, **F5** and **F6** with electron-donating groups on the ring A. However, introduction of 3-OH, $3-NH_2$, and $3-N_3$ groups on the ring A could significantly enhance the antiproliferative activity compared with other compounds against MGC-803 cells with IC_{50} values less than 1.0 μM. These inhibitory results suggested that substituent groups on the phenyl ring A exhibited a significant effect for the antiproliferative efficacy.

Based on compound **F10** and the SAR analysis, the effects of substituted benzothiazoles (ring B) on activity were further explored (https://www.sciencedirect.com/science/article/pii/S022352341830 9280 - tbl3 Table 1). Compounds **F11- F14** retained potent *in vitro* antiproliferative efficacy on MGC-803 cells with IC_{50} values less than 0.5 μM, and HCT-116 cells with IC_{50} values less than 4.0 μM. Compared compound **F10** with compounds **F11- F14**, substituted benzothiazoles of ring B might slightly impair antiproliferative activity than without substituted groups of ring B against tested cancer cells.

With compound **F10** in hand, we then performed further SARs studies (Table 2). In this series of target compounds, we explored the importance of the 3-hydroxyl group of A ring. These antiproliferative efficacy results suggested that 4-methoxy group on ring A had significant effect on antiproliferative activity. When the 4-methoxy group of ring A was replaced by other groups ($4-CH_3$, 4-F, 4-Cl, 4-Br, and 4-H), compounds **J1**-**J5** exhibited poorer activity (almost IC_{50} values > 40 μM) compared with compound **F10**. However, compound **J6** with a 4-methoxy group on ring A showed decent activity against MGC-803 and HCT-116 cells with IC_{50} values of 0.163 μM and 0.426 μM, which were lower than compound **F10** with 3-hydroxyl group and 4-methoxy groups of A ring. The *in vitro* antiproliferative efficacy results indicated the 4-methoxy group on the ring A plays a significant role in antiproliferative activity and introduction of 3-OH and $3-NH_2$ groups can significantly enhance

Table 2
Antiproliferative activity of compounds **J1-J6** against MGC-803, HCT-116 and PC-3 cells.

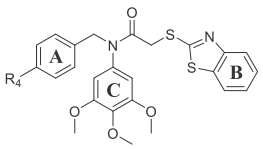

Compound	R4	IC_{50} (μmol/L)[a]		
		MGC-803	HCT-116	PC-3
J1	H	44.3 ± 2.59	54.5 ± 1.94	54.1 ± 2.14
J2	-F	>80	59.8 ± 1.93	50.82 ± 1.86
J3	-Cl	>80	60.3 ± 1.34	>80
J4	-Br	48.1 ± 5.18	63.8 ± 1.96	>80
J5	$-CH_3$	54.2 ± 12.4	>80	>80
J6	$-OCH_3$	0.163 ± 0.032	0.426 ± 0.022	8.46 ± 1.78
5-FU	–	6.82 ± 1.17	13.8 ± 1.96	18.4 ± 1.73
Colchicine	–	0.107 ± 0.010	0.129 ± 0.020	0.338 ± 0.014
CA-4P	–	0.020 ± 0.002	0.042 ± 0.006	0.033 ± 0.004

[a] Antiproliferative activity was assayed by exposure for 48 h.

the *in vitro* antiproliferative activity.

Based on above inhibitory activity results and SARs analysis, we conclude that 4-methoxy group on the ring A plays a significant role in antiproliferative activity and introduction of 3-OH, 3-NH_2, and 3-N_3 groups could significantly enhance the antiproliferative activity. The antiproliferative efficacy of target compounds varies with its substituent groups on the ring A. Substituted benzothiazoles of B ring may slightly impair antiproliferative activity against tested cancer cells compared with compound **F10**. The SARs of target compounds were summarized in Fig. 3.

3.2. Compound F10 selectively inhibits gastric cancer cells

The most active compound **F10** was selected to do the mechanism studies according to above inhibitory activity results. SGC-7901 and GES-1 cells were used to detect the selective inhibition of compound **F10**. The 48 h IC_{50} values of MGC-803, SGC-7901 and GES-1 cells were 0.035 μM, 0.049 μM and 0.249 μM, respectively (Fig. 4B). As shown in Fig. 4A, compound **F10** dose-dependently inhibited MGC-803 and SGC-7901 cells. With high dose treatment of compound **F10**, the inhibition rates of MGC-803 and SGC-7901 cells respectively were 72% and 63% while its inhibition rate of GES-1 were under 20%. Results in Fig. 4C&D showed compound **F10** inhibited MGC-803 and SGC-7901 cells growth in dose and time-dependent manners. These results suggested compound **F10** selectively inhibited gastric cancer cells and showed much a lower toxicity against normal gastric cell lines GES-1. Therefore, Compound **F10** was selected to do the further study for its high inhibition activity against MGC-803 and SGC-7901 cells.

Moreover, we detected the effects of compound **F10** on drug resistance at cell levels. As shown in Fig. 4E, paclitaxel (PTX) resistant MGC-803 cells were less sensitive to PTX than regular MGC-803 cells. The IC_{50} of PTX against MGC-803 was 8.11 nM, while IC_{50} against MGC-803/PTX was 88.68 nM. Therefore, the PTX resistance Index of MGC-803/PTX is 10.93. With pre-incubation of compound **F10** (15 nM, 48 h inhibition rate against MGC-803/PTX <15%) for 24 h, the IC_{50} of PTX against MGC-803/PTX was reduced from 88.68 nM to 45.22 nM (Fig. 4F). This result illustrated that compound **F10** could rescue the PTX resistant on MGC-803 cells.

3.3. Compound F10 inhibited tubulin polymerization in vitro

Since this series of compounds were designed as tubulin polymerization inhibitor, the inhibiting polymerization activity of tubulin was first to be verified. The *in vitro* tubulin polymerization inhibition activity was evaluated for compound **F10** and colchicine (as a positive control group) at different concentrations. As shown in Fig. 5D, the results suggested that compound **F10** and colchicine produced a dose-dependent inhibition of tubulin polymerization and gave IC_{50} values 1.9 μM and 7.5 μM, respectively. As shown in Fig. 5B, these results are consistent with the observed higher potency of compound **F10** in antiproliferative activity and tubulin polymerization than that of colchicine. EBI (N,N′-ethylenebis(iodoacetamide)) can alkylate β-tubulin when its colchicine binding site is free. Compound **F10** down regulated tubulin adduct in a dose-dependent manner (Fig. 5C), which indicated compound **F10** could competitively bind to the colchicine binding site of β-tubulin. 2 gastric cancer cell lines were stained and observed using microscope after treated with compound **F10**, the mid and high dose group of compound **F10** prevented the polymerization of tubulin from formatting microtubule which is a major component of the cytoskeleton and actor of mitosis. β-tubulin did not form a filamentous structure, instead they appeared dotted. Multiple nucleus was observed as the result of failed in mitosis (Fig. 5A). These results indicated that compound **F10** could as a novel anti-tubulin polymerization agent targeting colchicine binding site, which lead to tubulin polymerization inhibition intracellular and extracellular.

3.4. Molecular docking study

To explore the binding mechanism of compound **F10** with tubulin, a molecular docking study was performed of compound **F10** into the colchicine binding pocket of β-tubulin (PDB ID: 6O61). The docking result showed that compound **F10** could well bind into the colchicine binding site of tubulin (Fig. 6). The 3,4,5-trimethoxyphenyl group could form an unconventional hydrogen bond with the side chain of Cys239, and the hydrogen bond distance was 1.9 Å. The 3-hydroxyl-4- methoxyphenyl could form two hydrogen bonds with the main chain of Leu246 and the side chain of Asn101. The hydrogen bonds distances were 1.6 Å and 2.0 Å, respectively. These two groups were also had hydrophobic interaction with Leu240, Leu246 and Lys252. The benzothiazole group was located in a hydrophobic pocket consist of Tyr200, Val236, Leu240, Leu250, Leu253 and Ile316. Meanwhile, the carbonyl group formed a hydrogen bond with the side chain of Asn256 in the distance of 1.9 Å. These interactions made compound **F10** tightly bind in the colchicine binding site and exhibit a strong polymerization inhibiting activity against tubulin.

3.5. Compound F10 inhibited proliferation of gastric cancer cells

Tubulin polymerization inhibition could lead to proliferation inhibition, cell cycle arrestment at G2/M phase to be specific. As shown in Fig. 7A, compound **F10** dose-dependently arrested 2 gastric cancer cells at G2/M phase. The percentage of G2/M cells with high dose treatment both 2 gastric cell lines rose to about 2 folds that of control group. Cell cycle arrestment would be embodied in activity of cell formatting colonies. With 7 days treatment with compound **F10**, cells' activities formatting colony were obviously inhibited (Fig. 7B). G2/M phase related proteins were detected next. As expected, M phase marker p-Histone $H3^{Ser10}$ was up regulated and G2 phase related proteins CyclinB1 and CDK1 were down regulated (Fig. 7C).

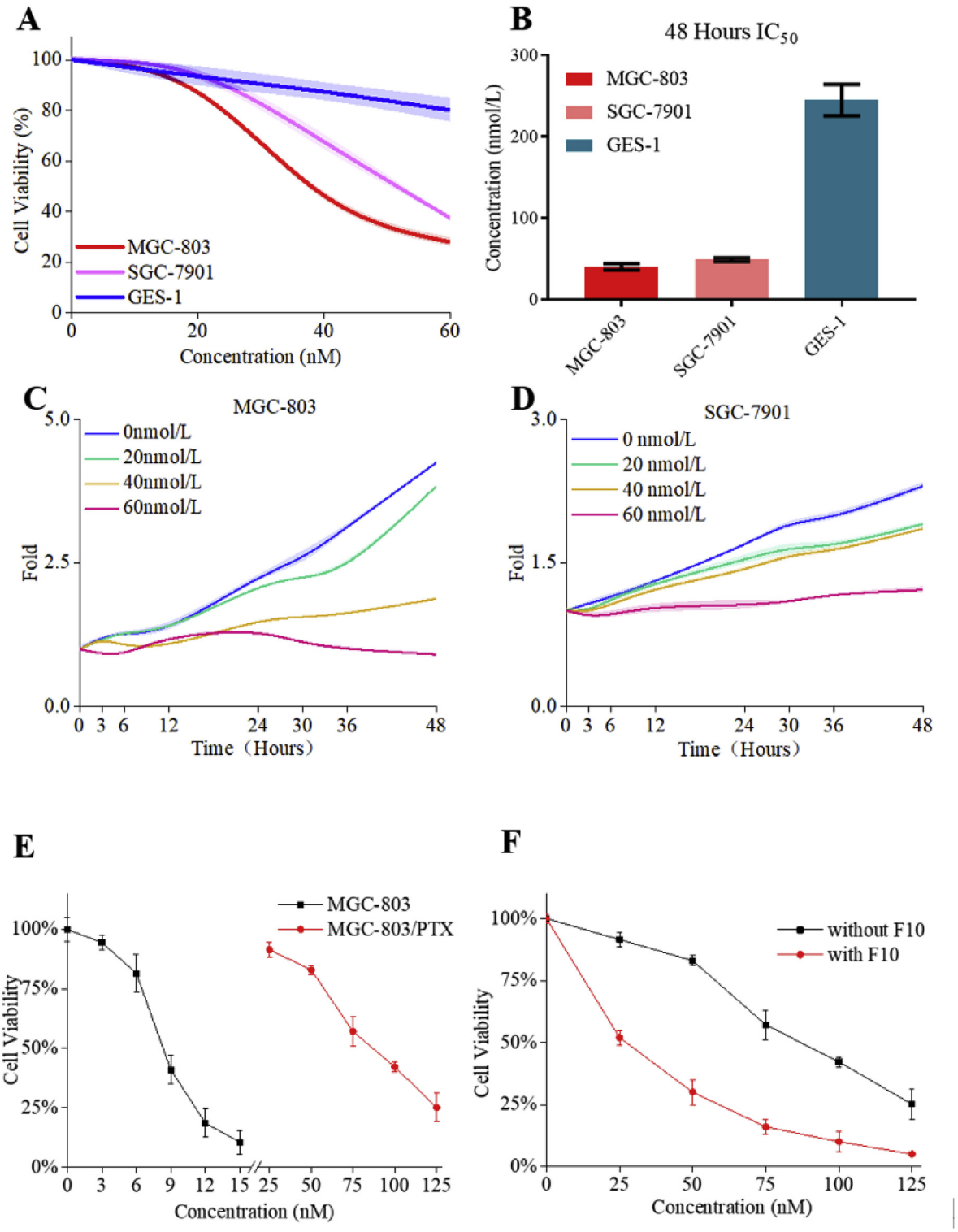

Fig. 4. Compound F10 selectively inhibited MGC-803 and SGC-7901 cells. Cells were incubated with 20, 40 and 60 nM F10 for 48 h. A. Cell viabilities of 3 gastric cell lines; B. The 48 h IC_{50} values of 3 gastric cell lines; C&D. Growth curves of 2 gastric cancer cell lines. E. Cell viabilities of MGC-803 and MGC-803/PTX cells. Cells were treated with PTX for 48 h. F. Cell viabilities of MGC-803/PTX. Cells were pre-incubated with or without 15 nM compound **F10** for 24 h, then treated with PTX for 48 h.

To sum up, compound **F10** arrested MGC-803 and SGC-7901 cells at G2/M phase and inhibited cell colony formatting resulting in proliferation inhibition in MGC-803 and SGC-7901 cells.

3.6. Compound F10 activated Hippo signaling pathway

Hippo signaling pathway plays an important role in tissue regeneration, organ size control, and cancer. In this work,

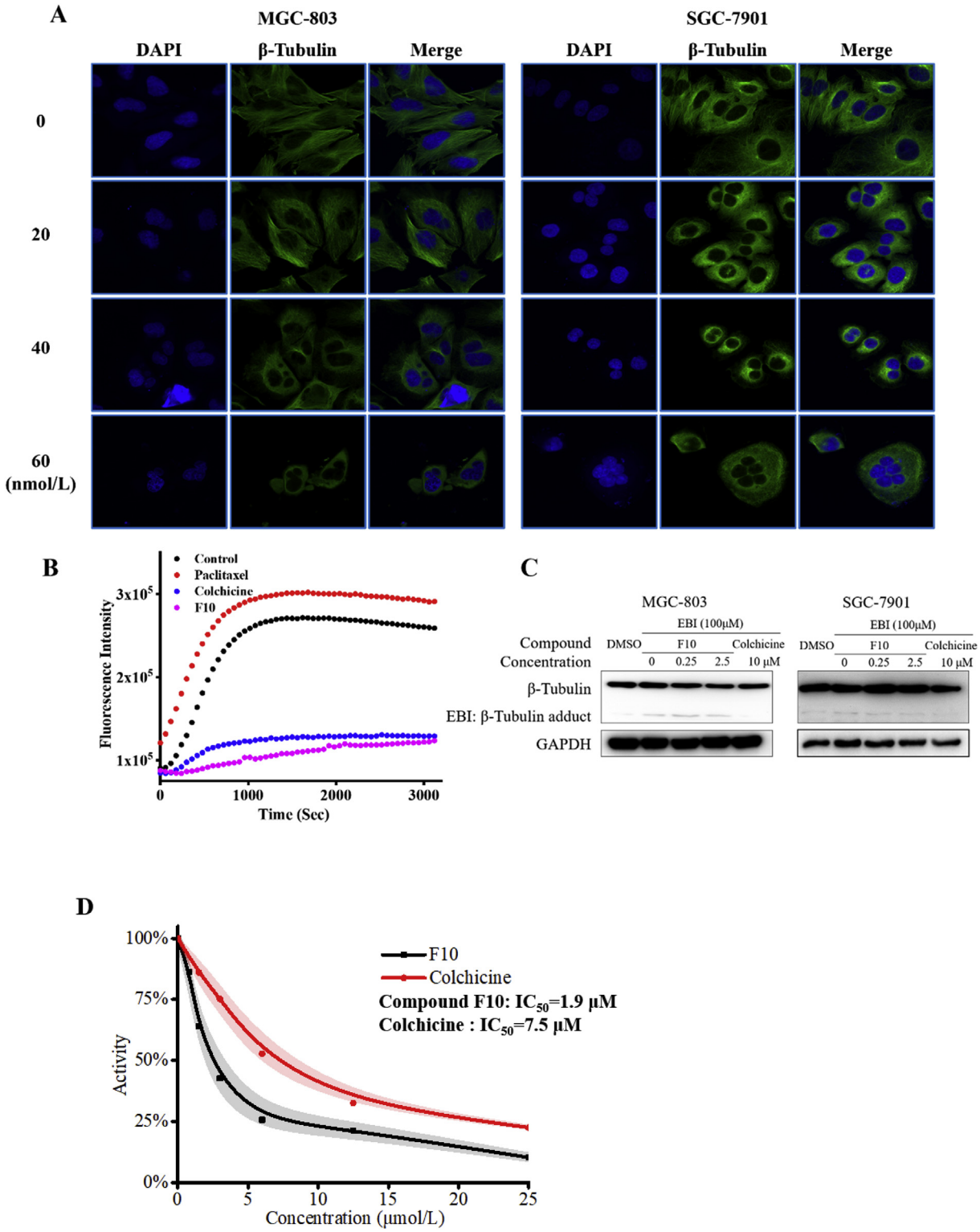

Fig. 5. Compound F10 inhibited tubulin polymerization *in vitro*. A. β-tubulin (green) nucleus (blue) in MGC-803 and SGC-7901 cells. Cells were incubated with 20, 40 and 60 nM F10 for 48 h; B. Tubulin polymerization extracellular, concentrations of Paclitaxel, Colchicine and F10 were 3 μmol/L; C. EBI competition assay on MGC-803 and SGC-7901 cells; D. Effects of F10 and colchicine on tubulin polymerization *in vitro*.

compound **F10** could effectively activated Hippo pathway and then lead to down-regulation of activated YAP. As shown in Fig. 7A, compound **F10** promoted phosphorylation of MST1/2 which was the upstream of Hippo. Increased p-MST1/2 promoted phosphorylation of its downstream protein LATS. p-LATS then caused inactivation (phosphorylation) of YAP protein. Activated YAP together with transcription factor TEAD express downstream proteins that contribute to surviving and proliferation. Besides inactivating YAP, compound **F10** also down regulated TEAD (Fig. 8A). c-Myc and Bcl-2 are 2 proteins regulated by YAP-TEAD

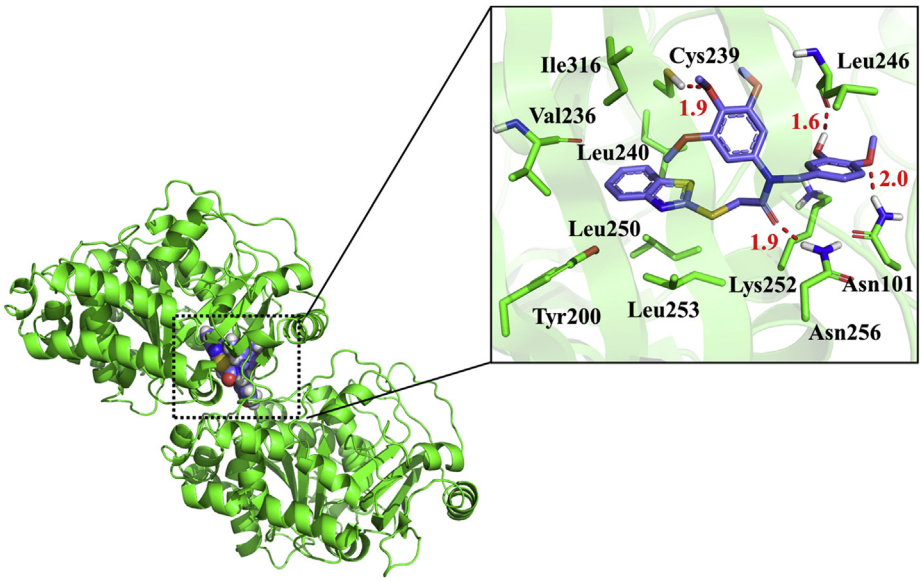

Fig. 6. The proposed binding mode of compound **F10** with tubulin (PDB ID: 6O61).

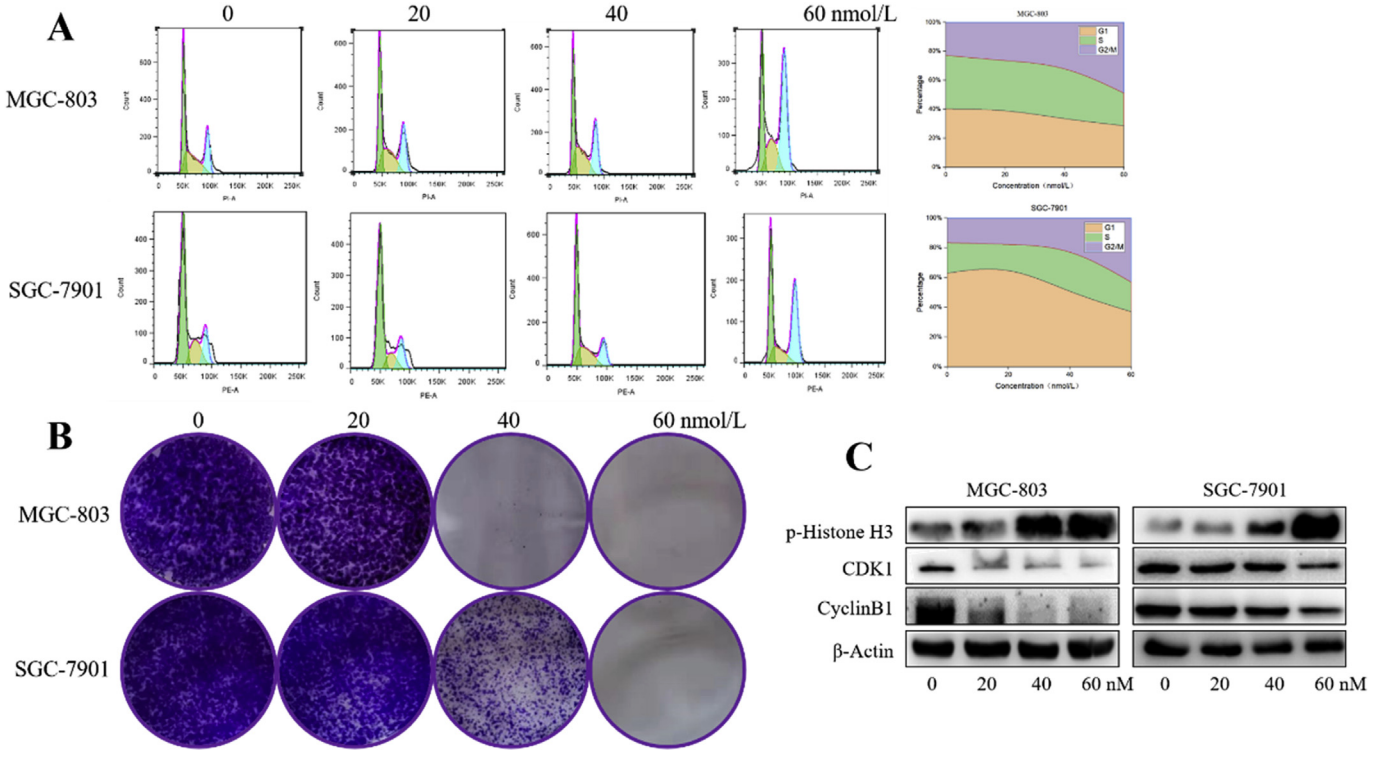

Fig. 7. Compound **F10** inhibited cell proliferation. A. Cell cycle analysis of 2 gastric cancer cell lines, cells were incubated with 20, 40 and 60 nM **F10** for 24 h; B. Colony formatting analysis, cells were incubated with 20, 40 and 60 nM **F10** for 7 days; C. Cell cycle related proteins in 2 cancer cell lines were detected by western blotting, cells were incubated with 20,40 and 60 nM **F10** for 48 h.

complex. Among them c-Myc is a proliferation and anti-apoptosis protein, Bcl-2 is an anti-apoptosis protein. The decrease of YAP and TEAD led to low expression of c-Myc and Bcl-2 (Fig. 8A). This cascade above was involved by compound **F10** in a dose-dependent manner. Next siRNA silencing was performed to downregulate YAP. The siYAP-1557 was the most effective one (Fig. 8B). For YAP silenced MGC-803 cell lines, the c-Myc and Bcl-2 decreases induced by compound **F10** were obviously rescued (Fig. 8C). The cell viability inhibitions caused by compound **F10** were also reversed when YAP silenced in both MGC-803 cell lines and SGC-7901 cell lines (Fig. 8D).

In conclusion, compound **F10** activated Hippo signaling pathway from its very beginning MST1/2, as the result of Hippo cascade YAP were inhibited. Which led to a decrease of c-Myc and

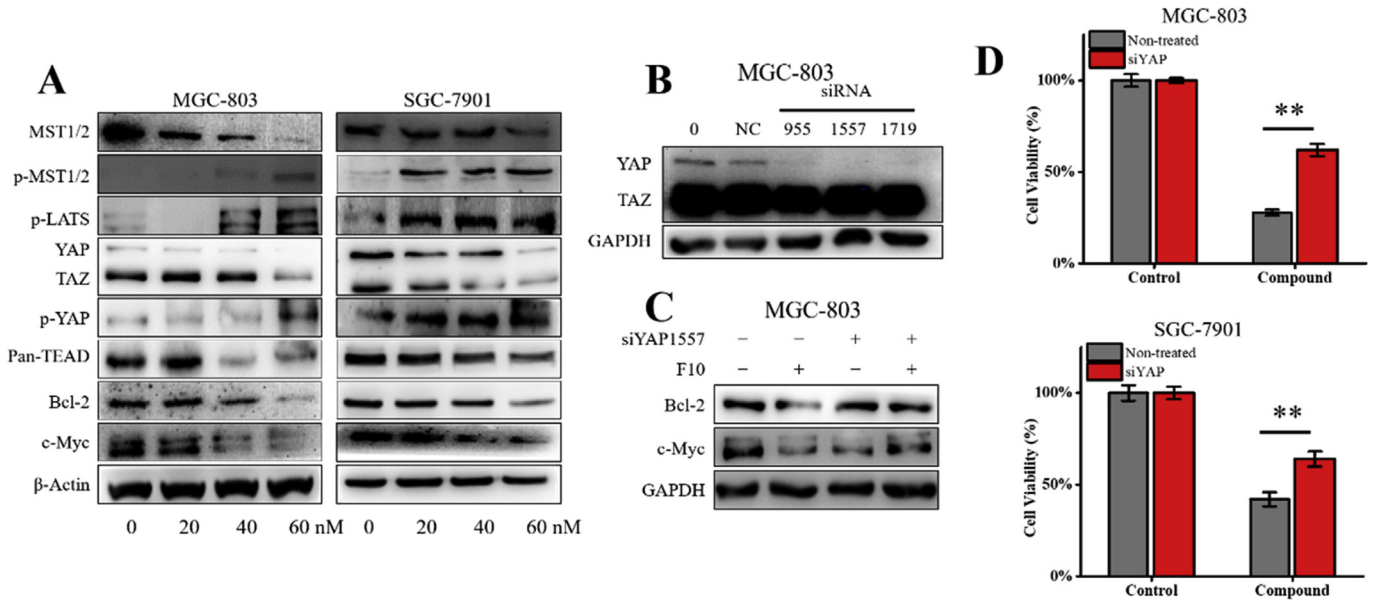

Fig. 8. Compound **F10** activated Hippo pathway. A. Hippo related proteins in 2 cancer cell lines, cells were incubated with 20,40 and 60 nM **F10** for 48 h; B. Effects of 3 siYAP on silencing YAP; C. Bcl-2 and c-Myc expression levels, MGC-803 cells were treated with siYAP-1557 and compound **F10** (60 nmol/L) for 48 h; D. Cell viabilities of 2 cancer cells, cells were treated with siYAP-1557 and compound **F10** (60 nmol/L) for 48 h.

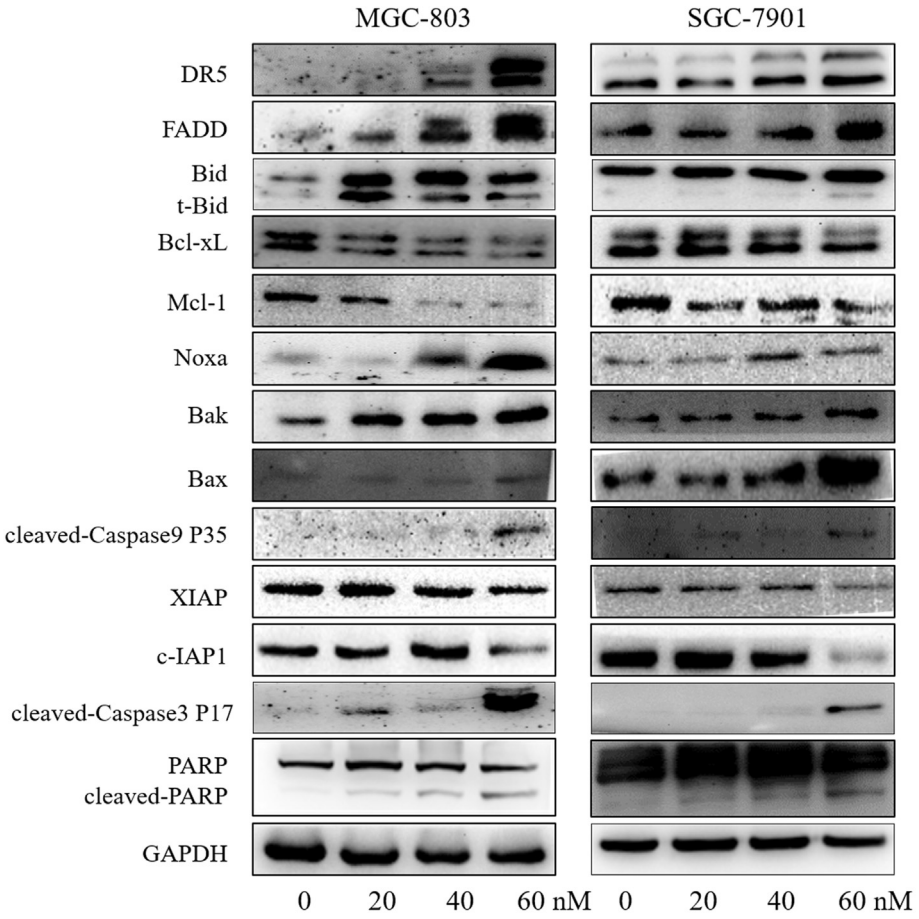

Fig. 9. Compound **F10** regulated apoptosis related proteins in 2 gastric cancer cell lines, cells incubated with 20, 40 and 60 nM **F10** for 48 h.

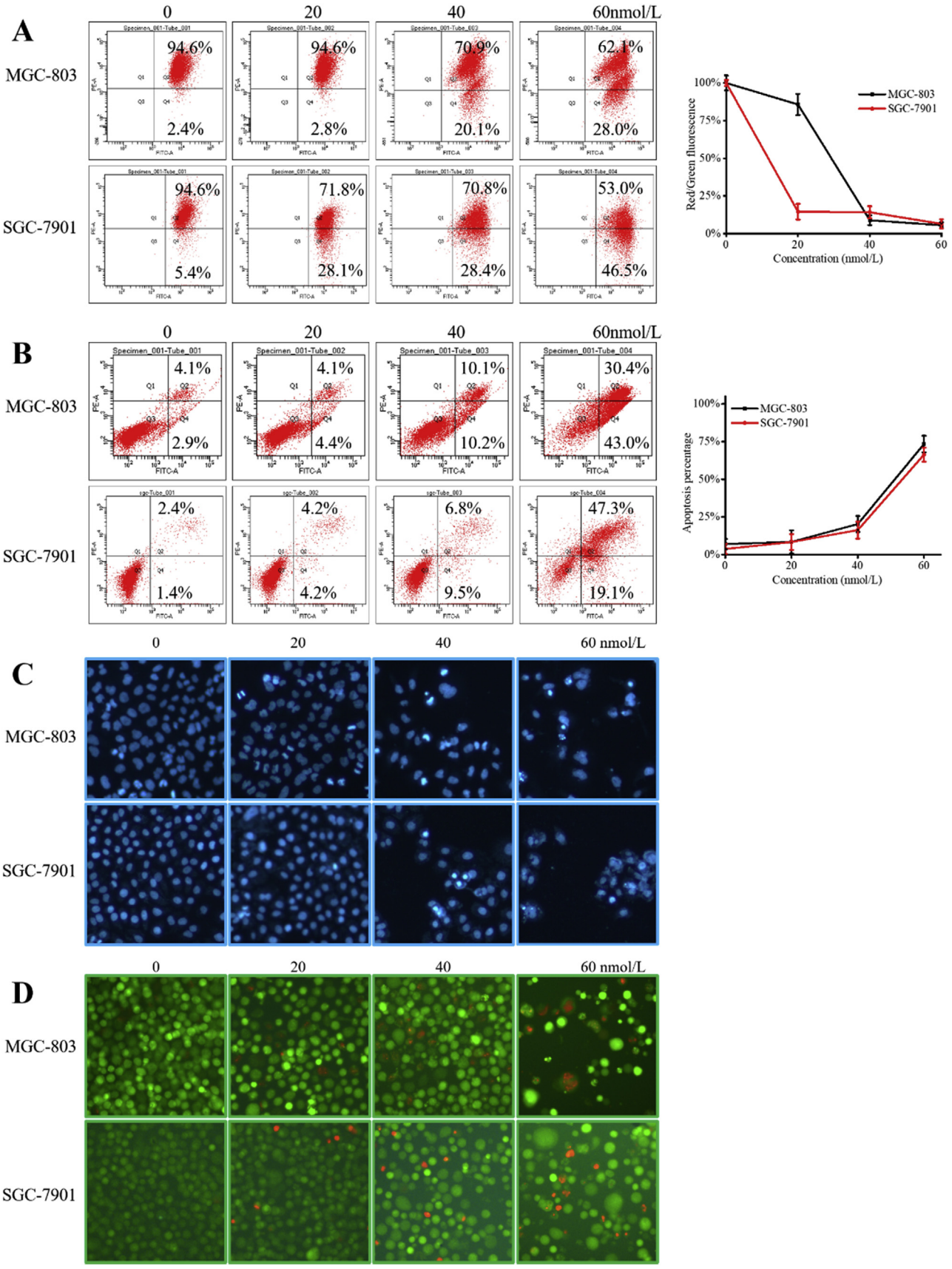

Fig. 10. Compound **F10** induced cell apoptosis in both 2 cell lines, cells were incubated with 20, 40 and 60 nM **F10** for 48 h in A, B and C. A. Depolarize of Mitochondrial membrane potential; B. Cell apoptosis analysis; C. Cell nucleus' morphological changes; D. Live-Dead cell stain, cells are divided into living cells (green) and dead cells (red), cells were t incubated with 20, 40 and 60 nM **F10** for 24 h. (For interpretation of the references to color in this figure legend, the reader is referred to the Web version of this article.)

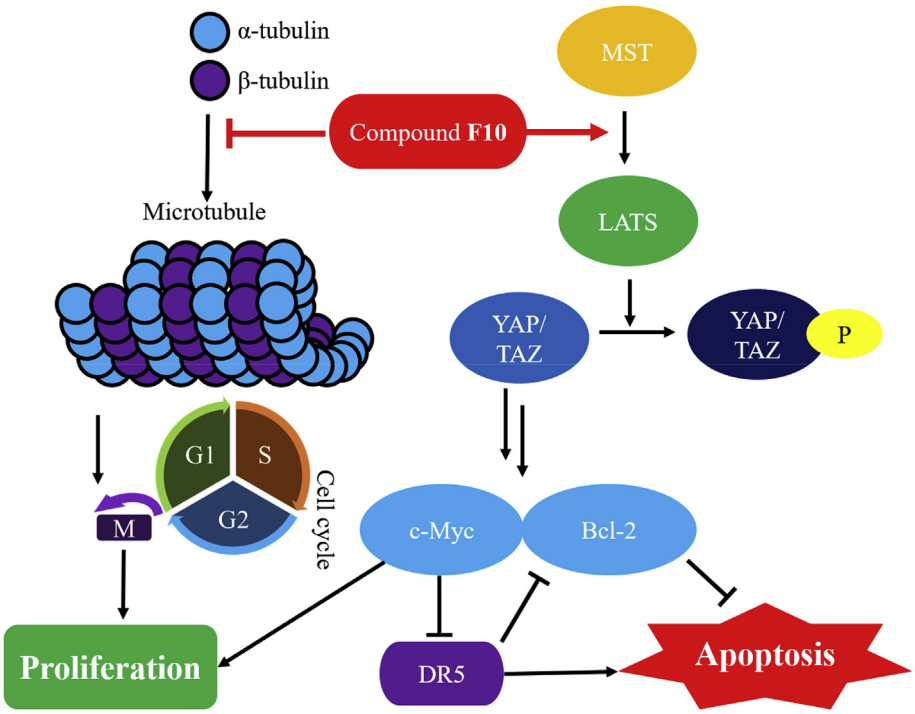

Fig. 11. Model of a mechanism by which compound **F10** inhibits tubulin polymerization and activates Hippo signaling pathway to inhibit gastric cancers.

Bcl-2 expression, the target genes of YAP. It was proved the down regulation of c-Myc, Bcl-2 led the inhibition of cell viabilities caused by compound **F10** were depend on its activity activating Hippo pathway.

3.7. *Compound F10 induced cell apoptosis*

Down regulation of c-Myc, Bcl-2 were the results of activation of Hippo induced by compound **F10**. The protein of c-Myc is a proliferation and anti-apoptosis protein. It has been reported that c-Myc negative regulates pro-apoptotic protein DR5 (Death Receptor 5), which can induce an extrinsic apoptosis. Bcl-2 is a well-known anti-apoptotic protein. The decrease of Bcl-2 could lead to an intrinsic apoptosis. As shown in Fig. 9, with the compound **F10** treatment on 2 gastric cancer cells, DR5 was up regulated. FADD, protein with DD domain which can be recruited by DR5 was up regulated. Their downstream t-Bid (activated Bid) was also up regulated. Anti-apoptosis proteins in Bcl-2 family Bcl-xL, Mcl-1 were decreased. Pro-apoptosis proteins in Bcl-2 family Noxa, Bak and Bax were increased (Fig. 9). Mitochondrial membrane potential depolarization is an important event of intrinsic apoptosis Bcl-2 family regulated. There occurs an obvious depolarize of mitochondrial membrane potential after compound **F10** treatment (Fig. 10A). XIAP and c-IAP1, 2 Inhibitor of Apoptosis Proteins, were down regulated by compound **F10**.2 Caspase family members Caspase3 and Caspase9 were evidently activated (cleaved). Their substrate PARP was also cleaved (Fig. 9). At cell level, cells were induced apoptosis by compound **F10**. Compound **F10** rose apoptosis percentages to 73% (MGC-803 cells) and 66% (SGC-7901 cells) from 7% to 4% (Fig. 10B). Apoptosis-like changes, like concentration and fragmentation, occurred in nucleus of 2 gastric cancer cells (Fig. 10C). With the concentration of F10 rises, more and more cells were induced dead (Fig. 10D).

The results show that compound regulated apoptosis related proteins then induced extrinsic and intrinsic apoptosis of gastric cancer cells.

4. Conclusion

In summary, novel tertiary amide derivatives incorporating benzothiazole moiety were explored via opening ring of β-lactam derivatives. *In vitro* Antiproliferative activity of compounds was evaluated for three human cancer cells. Some of them displayed potent antiproliferative efficacy and compound **F10** showed excellent antiproliferative activity against MGC-803 cells (IC_{50} = 0.035 μM), HCT-116 cells (IC_{50} = 0.182 μM), PC-3 cells (IC_{50} = 2.11 μM) and SGC-7901 cells (IC_{50} = 0.049 μM), respectively. In addition, the SARs of the synthesized compounds were studied and summarized.

In further study, the results of *in vitro* tubulin polymerization inhibitory assay and EBI alkylate assay suggested compound **F10** effectively inhibited tubulin polymerization binding to colchicine site with an IC_{50} value of 1.9 μM. And also, compound **F10** exhibited a strong activity against tubulin polymerization intracellular and extracellular. Molecular docking results suggested compound **F10** could bind tightly into the colchicine binding site of tubulin. Further molecular experiments indicated that compound **F10** arrested MGC-803 and SGC-7901 cells at G2/M phase and inhibited cell colony formatting (Fig. 11). On the other hand, compound **F10** activated Hippo signaling pathway to inactive the YAP protein. Then down regulated Bcl-2 and c-Myc depend on YAP inactivation. Then compound **F10** induced extrinsic and intrinsic apoptosis of 2 gastric cancer cells (Fig. 11). As the result of proliferation inhibition and apoptosis inducement compound **F10** selectively inhibited gastric cancer cells.

Here, compound **F10** was the first to be reported as a new anticancer agent *in vitro* via inhibiting β-tubulin polymerization and activating the Hippo signaling pathway.

5. General

In this work, commercial materials were purchased from reagent companies (Beijing Innochem Science &Technology Co. Ltd

and Zhengzhou HeQi Compony). We used an X-5 micromelting apparatus (Hanon Compony) to determine the melting points. NMR spectra was recorded on a Bruker spectrometer. HRMS spectra was recorded on a Waters Micromass spectrometer by ESI.

5.1. Synthesis of compounds C1-C10, D1-D10 and E1-E12

A solution of various aromatic aldehydes **A1-A10** (1.0 mmol, 1.0 eq) and 3,4,5-trimethoxyaniline (1.0 mmol, 1.0 eq) were added into EtOH (20 ml) at 80 °C for 6 h. When the reactions were complete, organic phases were collected to give crude the products **C1-C10** without further purified with column chromatography.

A solution of compounds **C1-C10** (1.0 mmol, 1.0 eq), benzoic acid (1.0 mmol, 1.0 eq) and $NaBH_4$ (1.0 mmol, 1.0 eq) were added into DCM (20 ml) at 25 °C for 8 h. When the reactions were complete, organic phases were collected to obtain crude products and then were purified by column chromatography to obtain compounds **D1-D10**.

A solution of compounds **D1-D10** (1.0 mmol, 1.0 eq) and acyl chloride derivatives (1.0 mmol, 1.0 eq) were added into DMF (8 ml) at 25 °C for 6–8 h. Then using EA (20 ml) extracted aqueous layers for three times. Collected organic layers were washed by saturated salt water, dried over magnesium sulfate anhydrous and evaporated to get crude products. Crude products were purified by column chromatography to obtain compounds **E1-E11**.

5.2. Synthesis of compounds F1-F14

A solution of compounds **E1-E11** (0.5 mmol, 1.0 eq), substituted benzothiazoles (0.6 mmol, 1.2 eq) and K_2CO_3 (0.75 mmol, 1.5 eq) were added into acetonitrile (10 ml) at 80 °C for 6 h. Upon completion, organic phase was collected to obtain crude products and then were purified with column chromatography to give compounds **F1-F14**.

2-(benzo[d]thiazol-2-ylthio)-N-(3-fluoro-4-methoxybenzyl)-N-(3,4,5-trimethoxyphenyl) acetamide(*F1*).

Yield, 49%, M.p. 118–119 °C, White solid.^{1}H NMR (400 MHz, DMSO-d_6) δ 8.00 (d, J = 7.9 Hz, 1H), 7.75 (d, J = 8.0 Hz, 1H), 7.46 (t, J = 7.6 Hz, 1H), 7.36 (t, J = 7.6 Hz, 1H), 7.13–6.96 (m, 3H), 6.69 (s, 2H), 4.83 (s, 2H), 4.26 (s, 2H), 3.80 (s, 3H), 3.71 (s, 6H), 3.66 (s, 3H). ^{13}C NMR (100 MHz, DMSO-d_6) δ 166.21, 153.05, 152.40, 149.94, 146.23, 137.04, 136.75, 134.65, 130.16, 130.11, 126.30, 124.53, 124.50, 124.45, 121.83, 115.65, 113.46, 106.00, 60.01, 56.01, 55.92, 51.66, 36.83. HR-MS (ESI): Calcd. $C_{26}H_{25}FN_2O_5S_2$, [M+H] $^+$ m/z: 529.1262, found: 529.1256.

2-(benzo[d]thiazol-2-ylthio)-N-(3-bromo-4-methoxybenzyl)-N-(3,4,5-trimethoxyphenyl) acetamide(*F2*).

Yield, 47%, M.p. 136–137 °C, White solid.^{1}H NMR (400 MHz, DMSO-d_6) δ 7.99 (d, J = 8.0 Hz, 1H), 7.75 (d, J = 8.0 Hz, 1H), 7.46 (d, J = 9.0 Hz, 2H), 7.36 (t, J = 7.6 Hz, 1H), 7.21 (d, J = 8.0 Hz, 1H), 6.99 (d, J = 8.4 Hz, 1H), 6.68 (s, 2H), 4.83 (s, 2H), 4.26 (s, 2H), 3.81 (s, 3H), 3.72 (s, 6H), 3.66 (s, 3H).^{13}C NMR (100 MHz, DMSO-d_6) δ 166.34, 166.00, 154.54, 153.05, 152.40, 137.04, 136.64, 134.64, 132.81, 130.87, 129.07, 126.30, 124.44, 121.80, 120.91, 112.28, 110.19, 106.07, 60.03, 56.14, 56.00, 51.34, 36.88. HR-MS (ESI): Calcd. $C_{26}H_{25}BrN_2O_5S_2$, [M+H] $^+$ m/z: 589.0461, found: 589.0455.

2-(benzo[d]thiazol-2-ylthio)-N-(4-methoxy-3-methylbenzyl)-N-(3,4,5-trimethoxyphenyl) acetamide(*F3*).

Yield, 61%, M.p. 136–138 °C, White solid. ^{1}H NMR (400 MHz, DMSO-d_6) δ 7.99 (d, J = 7.9 Hz, 1H), 7.73 (d, J = 8.0 Hz, 1H), 7.45 (t, J = 7.5 Hz, 1H), 7.35 (t, J = 7.5 Hz, 1H), 7.01 (s, 2H), 6.79 (d, J = 8.7 Hz, 1H), 6.65 (s, 2H), 4.80 (s, 2H), 4.25 (s, 2H), 3.74 (s, 3H), 3.70 (s, 6H), 3.66 (s, 3H).^{13}C NMR (100 MHz, DMSO-d_6) δ 166.11, 166.05, 156.51, 152.98, 152.43, 137.00, 136.85, 134.66, 130.51, 128.68, 127.07, 126.28, 125.23, 124.42, 121.79, 120.87, 109.81, 106.11, 60.01, 55.96, 55.14, 51.98, 36.94, 15.92. HR-MS (ESI): Calcd. $C_{27}H_{28}N_2O_5S_2$, [M+H] $^+$ 525.1512, found: 525.1508.

2-(benzo[d]thiazol-2-ylthio)-N-(4-methoxy-3-(trifluoromethyl)benzyl)-N-(3,4,5-trimethoxyphenyl) acetamide(*F4*).

Yield, 57%, M.p. 159–160 °C, White solid. ^{1}H NMR (400 MHz, DMSO-d_6) δ 7.99 (d, J = 7.9 Hz, 1H), 7.72 (d, J = 8.0 Hz, 1H), 7.48 (dd, J = 18.4, 10.1 Hz, 3H), 7.36 (t, J = 7.6 Hz, 1H), 7.15 (d, J = 8.5 Hz, 1H), 6.66 (s, 2H), 4.89 (s, 2H), 4.25 (s, 2H), 3.86 (s, 3H), 3.68 (d, J = 20.7 Hz, 9H). ^{13}C NMR (100 MHz, DMSO-d_6) δ 166.37, 165.98, 156.23, 153.08, 152.40, 137.08, 136.60, 134.63, 134.36, 129.15, 126.89, 126.85, 126.28, 124.44, 121.80, 120.84, 116.32, 112.69, 106.07, 60.01, 56.10, 55.93, 51.52, 36.86. HR-MS (ESI): Calcd. $C_{27}H_{25}F_3N_2O_5S_2$, [M+H]$^+$ m/z: 579.1230, found: 579.1224.

2-(benzo[d]thiazol-2-ylthio)-N-(3,4-dimethoxybenzyl)-N-(3,4,5-trimethoxyphenyl) acetamide(*F5*).

Yield, 49%, M.p. 121–123 °C, White solid.^{1}H NMR (400 MHz, DMSO-d_6) δ 7.59 (dd, J = 17.1, 7.3 Hz, 2H), 7.34–7.28 (m, 2H), 6.84 (d, J = 8.1 Hz, 1H), 6.80–6.74 (m, 2H), 6.67 (s, 2H), 4.82 (s, 2H), 4.27 (s, 2H), 3.71 (s, 9H), 3.67 (s, 3H), 3.64 (s, 3H).^{13}C NMR (100 MHz, DMSO-d_6) δ 166.08, 163.98, 152.98, 151.14, 148.46, 148.05, 141.10, 136.99, 136.60, 129.39, 124.61, 124.26, 120.75, 118.06, 112.13, 111.44, 110.10, 106.10, 60.02, 55.94, 55.44, 55.34, 52.34, 36.39. HR-MS (ESI): Calcd. $C_{27}H_{28}N_2O_6S_2$, [M+H] $^+$ m/z: 563.1281, found: 563.1244.

2-(benzo[d]thiazol-2-ylthio)-N-(3,4,5-trimethoxybenzyl)-N-(3,4,5-trimethoxyphenyl) acetamide(*F6*).

Yield, 44%, M.p. 149–150 °C, White solid.^{1}H NMR (400 MHz, DMSO-d_6) δ 7.99 (d, J = 7.9 Hz, 1H), 7.72 (d, J = 8.1 Hz, 1H), 7.44 (t, J = 7.6 Hz, 1H), 7.36 (t, J = 7.6 Hz, 1H), 6.69 (s, 2H), 6.50 (s, 2H), 4.83 (s, 2H), 4.29 (s, 2H), 3.72 (s, 6H), 3.64 (d, J = 11.6 Hz, 12H).^{13}C NMR (100 MHz, DMSO-d_6) δ 166.35, 166.01, 152.98, 152.65, 152.41, 137.02, 136.74, 136.64, 134.59, 132.84, 126.33, 124.47, 121.78, 120.83, 106.09, 105.67, 60.02, 59.97, 55.97, 55.75, 52.60, 36.99. HR-MS (ESI): Calcd. $C_{28}H_{30}N_2O_7S_2$, [M+H] $^+$ m/z: 571.1567, found: 571.1562.

2-(benzo[d]thiazol-2-ylthio)-N-(4-methoxy-3-nitrobenzyl)-N-(3,4,5-trimethoxyphenyl) acetamide(*F7*).

Yield, 61%, M.p. 147–148 °C, White solid. ^{1}H NMR (400 MHz, DMSO-d_6) δ 7.99 (d, J = 7.7 Hz, 1H), 7.78–7.70 (m, 2H), 7.53 (d, J = 8.3 Hz, 1H), 7.45 (t, J = 7.1 Hz, 1H), 7.35 (t, J = 7.5 Hz, 1H), 7.24 (d, J = 8.7 Hz, 1H), 6.73 (s, 2H), 4.91 (s, 2H), 4.27 (s, 2H), 3.89 (s, 3H), 3.73 (s, 6H), 3.66 (s, 3H). ^{13}C NMR (100 MHz, DMSO-d_6) δ 166.56, 165.97, 153.13, 152.38, 151.05, 138.90, 137.07, 136.58, 134.62, 134.30, 129.64, 126.31, 124.55, 124.45, 121.79, 120.80, 114.06, 106.02, 60.01, 56.61, 56.00, 51.21, 36.84. HR-MS (ESI): Calcd. $C_{26}H_{25}N_3O_7S_2$, [M+H]$^+$ m/z: 556.1207, found: 556.1201.

N-(3-azido-4-methoxybenzyl)-2-(benzo[d]thiazol-2-ylthio)-N-(3,4,5-trimethoxyphenyl) acetamide(*F8*).

Yield, 55%, M.p. 121–122 °C, White solid. ^{1}H NMR (400 MHz, DMSO-d_6) δ 7.99 (d, J = 7.8 Hz, 1H), 7.73 (d, J = 8.0 Hz, 1H), 7.46 (t, J = 7.5 Hz, 1H), 7.36 (t, J = 7.4 Hz, 1H), 7.04–6.89 (m, 3H), 6.68 (s, 2H), 4.81 (s, 2H), 4.25 (s, 2H), 3.81 (s, 3H), 3.72 (s, 6H), 3.66 (s, 3H).^{13}C NMR (100 MHz, DMSO-d_6) δ 166.33, 165.99, 153.05, 152.39, 151.14, 137.04, 136.79, 134.67, 130.38, 126.84, 126.24, 126.16, 124.43, 121.80, 120.85, 120.59, 112.41, 106.02, 60.02, 56.01, 51.70, 36.80. HR-MS (ESI): Calcd. $C_{26}H_{25}N_5O_5S_2$, [M+H] $^+$ m/z:552.1370, found: 552.1365.

N-(3-amino-4-methoxybenzyl)-2-(benzo[d]thiazol-2-ylthio)-N-(3,4,5-trimethoxyphenyl) acetamide(*F9*).

Yield, 63%, M.p. 149–150 °C, White solid.^{1}H NMR (400 MHz, DMSO-d_6) δ 8.00 (d, J = 7.9 Hz, 1H), 7.77 (d, J = 8.0 Hz, 1H), 7.46 (t, J = 7.5 Hz, 1H), 7.36 (t, J = 7.5 Hz, 1H), 6.71–6.59 (m, 3H), 6.55 (s, 1H), 6.39 (d, J = 7.7 Hz, 1H), 4.68 (d, J = 19.2 Hz, 4H), 4.24 (s, 2H), 3.71 (d, J = 8.1 Hz, 9H), 3.66 (s, 3H).^{13}C NMR (100 MHz, DMSO-d_6) δ 166.05, 165.94, 152.92, 152.42, 145.62, 137.28, 136.96, 136.85, 134.63, 129.44, 126.32, 124.44, 121.79, 120.93, 116.35, 113.99, 110.15, 106.09, 60.02,

55.95, 55.26, 52.35, 36.99. HR-MS (ESI): Calcd. $C_{26}H_{26}N_2O_6S_2$, $[M+H]^+$ *m/z*:526.1465, found: 526.1460.

2-(benzo[d]thiazol-2-ylthio)-N-(3-hydroxy-4-methoxybenzyl)-N-(3,4,5-trimethoxyphenyl) acetamide(*F10*).

Yield, 52%, M.p. 140–141 °C, White solid.^{1}H NMR (400 MHz, DMSO-d_6) δ 8.90 (s, 1H), 7.99 (d, *J* = 7.9 Hz, 1H), 7.77 (d, *J* = 8.0 Hz, 1H), 7.46 (t, *J* = 7.5 Hz, 1H), 7.36 (t, *J* = 7.5 Hz, 1H), 6.79 (d, *J* = 8.2 Hz, 1H), 6.70 (s, 1H), 6.61 (d, *J* = 8.1 Hz, 3H), 4.74 (s, 2H), 4.24 (s, 2H), 3.73 (s, 3H), 3.70 (s, 6H), 3.66 (s, 3H).^{13}C NMR (100 MHz, DMSO-d_6) δ 166.07, 166.02, 152.95, 152.40, 146.88, 146.21, 136.97, 136.78, 134.62, 129.70, 126.32, 124.46, 121.77, 120.93, 119.30, 115.79, 111.86, 106.05, 60.03, 55.95, 55.58, 52.11, 36.86. HR-MS (ESI): Calcd. $C_{26}H_{26}N_2O_6S_2$, $[M+H]^+$ *m/z*: 527.1305, found: 527.1300.

N-(3-hydroxy-4-methoxybenzyl)-2-((4-methylbenzo[d]thiazol-2-yl)thio)-N-(3,4,5-trimethoxyphenyl)acetamide(*F11*).

Yield, 42%, M.p. 150–151 °C, White solid.^{1}H NMR (400 MHz, DMSO-d_6) δ 8.90 (s, 1H), 7.78 (d, *J* = 6.4 Hz, 1H), 7.24 (d, *J* = 6.7 Hz, 2H), 6.78 (d, *J* = 8.0 Hz, 1H), 6.70 (s, 1H), 6.57 (s, 3H), 4.74 (s, 2H), 4.29 (s, 2H), 3.71 (d, *J* = 11.9 Hz, 9H), 3.64 (s, 3H).^{13}C NMR (100 MHz, DMSO-d_6) δ 166.02, 164.58, 152.99, 151.54, 146.92, 146.27, 137.01, 136.76, 134.40, 130.46, 129.76, 126.72, 124.37, 119.36, 119.09, 115.85, 111.87, 105.96, 59.98, 55.95, 55.59, 52.00, 37.20, 17.62. HR-MS (ESI): Calcd. $C_{27}H_{28}N_2O_6S_2$, $[M+Na]^+$ *m/z*: 563.1281, found: 563.1276.

2-((5-chlorobenzo[d]thiazol-2-yl)thio)-N-(3-hydroxy-4-methoxybenzyl)-N-(3,4,5-trimethoxyphenyl)acetamide(*F12*).

Yield, 59%, M.p. 142–144 °C, White solid.^{1}H NMR (400 MHz, DMSO-d_6) δ 8.91 (s, 1H), 8.14 (s, 1H), 7.74 (d, *J* = 8.6 Hz, 1H), 7.48 (d, *J* = 8.6 Hz, 1H), 6.80 (d, *J* = 8.1 Hz, 1H), 6.71 (s, 1H), 6.61 (d, *J* = 7.8 Hz, 3H), 4.75 (s, 2H), 4.25 (s, 2H), 3.74 (s, 3H), 3.71 (s, 6H), 3.67 (s, 3H).^{13}C NMR (100 MHz, DMSO-d_6) δ 167.42, 165.93, 152.97, 151.24, 146.91, 146.25, 137.01, 136.75, 136.21, 129.72, 128.80, 126.68, 121.95, 121.47, 119.32, 115.84, 111.86, 106.06, 60.02, 55.96, 55.58, 52.14, 37.08. HR-MS (ESI): Calcd. $C_{26}H_{25}ClN_2O_6S_2$, $[M+Na]^+$ *m/z*: 583.0735, found: 583.0729.

2-((5-bromobenzo[d]thiazol-2-yl)thio)-N-(3-hydroxy-4-methoxybenzyl)-N-(3,4,5-trimethoxyphenyl)acetamide(*F13*).

Yield, 46%, M.p. 136–137 °C, White solid.^{1}H NMR (400 MHz, DMSO-d_6) δ 8.90 (s, 1H), 7.99–7.91 (m, 2H), 7.52 (d, *J* = 8.5 Hz, 1H), 6.79 (d, *J* = 8.1 Hz, 1H), 6.68 (s, 1H), 6.61 (s, 3H), 4.74 (s, 2H), 4.23 (s, 2H), 3.73 (s, 3H), 3.70 (s, 6H), 3.66 (s, 3H).^{13}C NMR (100 MHz, DMSO-d_6) δ 168.80, 165.93, 153.61, 152.94, 146.90, 146.22, 136.98, 136.76, 133.94, 129.73, 127.04, 123.57, 123.29, 119.25, 119.14, 115.88, 111.80, 106.07, 60.02, 55.93, 55.59, 52.11, 37.02. HR-MS (ESI): Calcd. $C_{26}H_{25}BrN_2O_6S_2$, $[M+Na]^+$ *m/z*: 605.0410, found: 605.0405.

N-(3-hydroxy-4-methoxybenzyl)-2-((6-methoxybenzo[d]thiazol-2-yl)thio)-N-(3,4,5-trimethoxyphenyl)acetamide(*F14*).

Yield, 68%, M.p. 142–144 °C, White solid.^{1}H NMR (400 MHz, DMSO-d_6) δ 8.90 (s, 1H), 7.66 (d, *J* = 8.9 Hz, 1H), 7.58 (s, 1H), 7.04 (d, *J* = 8.9 Hz, 1H), 6.79 (d, *J* = 8.1 Hz, 1H), 6.70 (s, 1H), 6.60 (s, 3H), 4.73 (s, 2H), 4.19 (s, 2H), 3.80 (s, 3H), 3.73 (s, 3H), 3.69 (s, 6H), 3.66 (s, 3H).^{13}C NMR (100 MHz, DMSO-d_6) δ 166.13, 162.54, 156.64, 152.94, 146.90, 146.89, 146.24, 136.97, 136.81, 136.12, 129.74, 121.47, 119.30, 115.82, 114.99, 111.86, 106.05, 104.87, 60.02, 55.94, 55.63, 55.57, 52.09, 36.95. HR-MS (ESI): Calcd. $C_{27}H_{28}N_2O_7S_2$, $[M+Na]^+$ *m/z*: 579.1230, found: 579.1224.

5.3. Synthesis of compounds H1-H6 and I1-I10

A solution of benzyl chloride derivatives **G1-G6** (1.0 mmol, 1.0 eq), 3,4,5-trimethoxyaniline **B** (1.0 mmol, 1.0 eq) and K_2CO_3 were added into DMF (20 ml) at 25 °C for 6 h. When the reactions were complete, 20 ml H_2O and 20 ml ethyl acetate (three times) were added into aqueous layers. Collected organic layers were washed by H_2O and brine successively, dried over magnesium sulfate anhydrous and then evaporated to get crude products. Crude products were purified by column chromatography to obtain compounds **H1-H6**.

A solution of compounds **H1-H6** (1.0 mmol, 1.0 eq) and chloroacetic chloride (1.0 mmol, 1.0 eq) were added into DMF (8 ml) at 20 °C for 6–8 h. When the reactions were complete, 20 ml H_2O and 20 ml ethyl acetate (three times) were added into aqueous layers. Combined organic layers were washed by H_2O and brine successively, dried over magnesium sulfate anhydrous and then evaporated to get crude products. The crude products were purified by column chromatography to obtain compounds **I1-I6**.

5.4. Synthesis of compounds J1-J6

A solution of compounds **I1-I6** (0.5 mmol, 1.0 eq), 2-mercaptobenzothiazole (0.6 mmol, 1.2 eq) and K_2CO_3 (0.75 mmol, 1.5 eq) were added into acetonitrile (10 ml) at 80 °C for 6 h. Upon completion, the organic phases were collected and dried under a vacuum to give crude the products and then were purified by column chromatography to give compounds **J1-J16**.

2-(benzo[d]thiazol-2-ylthio)-N-benzyl-N-(3,4,5-trimethoxyphenyl) acetamide (*J1*).

Yield, 45%, M.p. 151–153 °C, White solid. ^{1}H NMR (400 MHz, $CDCl_3$) δ 7.65 (dd, *J* = 14.2, 8.0 Hz, 2H), 7.33–7.28 (m, 1H), 7.24–7.19 (m, 2H), 7.18 (d, *J* = 1.5 Hz, 4H), 6.25 (s, 2H), 4.83 (s, 2H), 4.00 (s, 2H), 3.74 (s, 3H), 3.62 (s, 6H). ^{13}C NMR (100 MHz, $CDCl_3$) δ 166.00, 164.62, 152.62, 151.85, 136.99, 136.18, 135.89, 134.55, 128.19, 127.42, 126.59, 124.93, 123.33, 120.28, 120.09, 104.80, 59.90, 55.15, 52.58, 35.62. HR-MS (ESI): Calcd. $C_{25}H_{24}N_2O_4S_2$, $[M+H]^+$*m/z*: 481.1250, found: 481.1257.

2-(benzo[d]thiazol-2-ylthio)-N-(4-fluorobenzyl)-N-(3,4,5-trimethoxyphenyl) acetamide(*J2*).

Yield, 60%, M.p. 145–146 °C, White solid.^{1}H NMR (400 MHz, $CDCl_3$) δ 7.67 (d, *J* = 7.9 Hz, 1H), 7.60 (d, *J* = 8.1 Hz, 1H), 7.35–7.28 (m, 1H), 7.25–7.21 (m, 1H), 7.15 (dd, *J* = 8.5, 5.5 Hz, 2H), 6.87 (t, *J* = 8.7 Hz, 2H), 6.27 (s, 2H), 4.79 (s, 2H), 3.98 (s, 2H), 3.75 (s, 3H), 3.65 (s, 6H).^{13}C NMR (101 MHz, $CDCl_3$) δ 166.04, 164.53, 152.70, 137.06, 135.82, 134.54, 132.04, 129.95, 129.87, 124.95, 123.37, 120.18, 120.12, 114.33, 114.12, 104.72, 59.91, 55.18, 51.88, 35.49. HR-MS (ESI): Calcd. $C_{25}H_{23}FN_2O_4S_2$, $[M+H]^+$ *m/z*: 499.1156, found: 499.1151.

2-(benzo[d]thiazol-2-ylthio)-N-(4-chlorobenzyl)-N-(3,4,5-trimethoxyphenyl) acetamide(*J3*).

Yield, 62%, M.p. 129–131 °C, White solid. ^{1}H NMR (400 MHz, CDCl3) δ 7.67 (d, *J* = 7.9 Hz, 1H), 7.57 (d, *J* = 8.0 Hz, 1H), 7.35–7.30 (m, 1H), 7.25–7.21 (m, 1H), 7.14 (q, *J* = 8.7 Hz, 4H), 6.29 (s, 2H), 4.79 (s, 2H), 3.98 (s, 2H), 3.75 (s, 3H), 3.66 (s, 6H). ^{13}C NMR (100 MHz, $CDCl_3$) δ 166.13, 164.48, 152.74, 151.77, 137.10, 135.84, 134.70, 134.55, 132.50, 129.58, 127.56, 124.98, 123.39, 120.18, 120.14, 104.70, 59.92, 55.22, 52.02, 35.42. HR-MS (ESI): Calcd. $C_{25}H_{23}ClN_2O_4S_2$, $[M+H]^+$ *m/z*: 515.0861, found: 515.0865.

2-(benzo[d]thiazol-2-ylthio)-N-(4-bromobenzyl)-N-(3,4,5-trimethoxyphenyl) acetamide(*J4*).

Yield, 49%, M.p. 134–135 °C, White solid.^{1}H NMR (400 MHz, $CDCl_3$) δ 7.68–7.65 (m, 1H), 7.56 (d, *J* = 7.8 Hz, 1H), 7.36–7.28 (m, 3H), 7.24–7.20 (m, 1H), 7.07 (d, *J* = 8.4 Hz, 2H), 6.29 (s, 2H), 4.77 (s, 2H), 3.97 (s, 2H), 3.75 (s, 3H), 3.65 (s, 6H).^{13}C NMR (100 MHz, $CDCl_3$) δ 161.86, 160.43, 148.52, 147.34, 132.89, 131.59, 130.97, 130.21, 126.30, 125.71, 120.82, 119.23, 116.40, 115.92, 100.48, 55.70, 51.01, 47.87, 31.26. HR-MS (ESI): Calcd. $C_{25}H_{23}BrN_2O_4S_2$, $[M+H]^+$ *m/z*: 559.0355, found: 559.0360.

2-(benzo[d]thiazol-2-ylthio)-N-(4-methylbenzyl)-N-(3,4,5-trimethoxyphenyl) acetamide(*J5*).

Yield, 52%, M.p. 150–153 °C, White solid.^{1}H NMR (400 MHz, $CDCl_3$) δ 7.64 (dd, *J* = 16.8, 8.0 Hz, 2H), 7.33–7.28 (m, 1H), 7.24–7.20 (m, 1H), 7.06 (d, *J* = 8.0 Hz, 2H), 6.99 (d, *J* = 7.9 Hz, 2H), 6.26 (s, 2H),

4.78 (s, 2H), 4.00 (s, 2H), 3.75 (s, 3H), 3.63 (s, 6H), 2.25 (s, 3H).^{13}C NMR (100 MHz, $CDCl_3$) δ 165.94, 164.76, 152.62, 151.75, 137.02, 136.23, 135.97, 134.49, 133.12, 128.19, 128.04, 124.93, 123.35, 120.30, 120.07, 104.89, 59.90, 55.17, 52.37, 35.70, 20.11. HR-MS (ESI): Calcd. $C_{26}H_{26}N_2O_4S_2$, $[M+H]^+$ *m/z*:495.1407, found: 495.1411.

2-(benzo[d]thiazol-2-ylthio)-N-(4-methoxybenzyl)-N-(3,4,5-trimethoxy phenyl) acetamide(*J6*).

Yield, 52%, M.p. 132–133 °C, White solid. ^{1}H NMR (400 MHz, $CDCl_3$) δ 7.64 (dd, *J* = 17.5, 8.0 Hz, 2H), 7.30 (t, *J* = 7.6 Hz, 1H), 7.22 (d, *J* = 7.5 Hz, 1H), 7.09 (d, *J* = 8.3 Hz, 2H), 6.71 (d, *J* = 8.3 Hz, 2H), 6.25 (s, 2H), 4.76 (s, 2H), 3.99 (s, 2H), 3.75 (s, 3H), 3.71 (s, 3H), 3.64 (s, 6H).^{13}C NMR (100 MHz, $CDCl_3$) δ 165.84, 164.77, 158.10, 152.62, 151.72, 136.98, 135.92, 134.48, 129.59, 128.35, 124.93, 123.36, 120.27, 120.09, 112.72, 104.87, 59.91, 55.20, 54.26, 52.02, 35.73. HR-MS (ESI): Calcd. $C_{26}H_{26}N_2O_5S_2$, $[M+H]^+$*m/z*:511.1356, found: 511.1360.

5.5. Cell culture

Cells were cultured in RPMI-1640 medium supplemented with 10% fetal bovine serum (FBS), 100 U/ml penicillin and 0.1 mg/ml streptomycin. All the cells were incubated at 37 °C and 5% CO2.

5.6. MTT assay

5,000 cells were seeded into 96-well cell culture plates. After 24 h, cells were treated with synthesized compounds. And then, MTT reagent was added 20 μL per well after 48 h treatment with synthesized compounds. Cells were then incubated for 4 h at 37 °C. Formazan was then dissolved with DMSO. Absorbencies of formazan solution at 490 nm were determined. SPSS version 10.0 was used for 50% inhibitory concentration (IC_{50}) calculation.

5.7. In vitro tubulin polymerization assay

Pig brain microtubule protein was isolated by three cycles of temperature-dependent assembly/disassembly in PIPES (pH 6.5, 100 mM), MgSO4 (1.0 mM), EGTA (2.0 mM), GTP (1.0 mM) and 2-mercaptoethanol (1.0 mM). In the first cycle of polymerization, glycerol and phenylmethylsulfonyl fluoride were added to 4 M and 0.2 mM, respectively. Homogeneous tubulin was prepared from microtubule protein by phosphocellulose (P11) chromatography. The purified proteins were stored in aliquots at −70 °C.

Tubulin protein was mixed with compound **F10** and colchicine in PEM buffer containing GTP (1 mM) and glycerol (5%). Microtubule polymerization was monitored by light scattering at 340 nm using a SPECTRA MAX 190(Molecular Device) spectrophotometer at 37 °C.

5.8. EBI alkylate assay

5×10^5 gastric cancer cells were seeded into 6-well cell culture plates. After 24 h, cells were treated with compound **F10**, colchicine and DMSO. After 2 h treatment, cells were then treated with 100 mmol/L EBI for another 2 h. At last, cells were harvested for the determine of β-tubulin and β-tubulin adduct (alkylated β-tubulin) with anti-β-tubulin antibody.

5.9. Molecular docking study

The molecular docking study was performed using MOE 2015.10. The crystal structure of Tubulin (PDB ID: 6O61) was retrieved from RCSB Protein Data Bank, and then was prepared by adding hydrogen atoms, removing water molecules and repairing the missing side chains. The protonation states of protein residues were calculated in the pKa at 7. The ligand compound **F10** was built in MOE 2015.10 and was prepared by energy minimization and conformational search. The ligands were docked into the colchicine binding site of tubulin and 20 poses were exported for the next analysis.

5.10. Western blot analysis

Gastric cancer cells were seeded in dishes and treated with compound **F10** or DMSO. After 48 h treatment, gastric cancers were collected and then lysed. The lysates of each group were electrophoretic separated in SDS-PAGE after denatured. Proteins were then transferred to PVDF membranes from the gel. After blocked, the membranes were incubated for 1st antibody conjugation. Then membranes were washed and incubated with 2nd antibody. The target proteins were detected after washed.

5.11. Gene silencing using small interfering RNA (siRNA)

Gastric cancer cells were seeded 5×10^5 cells per dish into 60-mm dishes and transfected with siRNA oligonucleotides (100 nmol/L), purchased from GenePharma (Shanghai, China) using Lipofectamine 2000 (Cat. No. 11668019, Thermo Fisher Scientific). Cells were transfected with siRNA for 48 h and further treated with compound for 48 h. The sequences of the siRNA are as follows:

5.12. General methods

Colony formation assay, cell apoptosis assay, cell cycle distribution assay, flow cytometry analysis, and immunostaining assay were proceeded according to our group reported work in European journal of medicinal chemistry [49] and Bioorganic & Medicinal Chemistry Letters [50].

5.13. Statistical analysis

The data of three independent experiments were expressed as mean ± SD and calculated by SPSS version 17.0.

Competing financial interests

There is no conflict of interest about this article to declare.

Declaration of competing interest

There is no conflict of interest about this article to declare.

Acknowledgement

This work was supported by the National Key Research Program of Proteins (No. 2016YFA0501800 for Hong min Liu, China), National Natural Science Foundation of China of China (No. 81703541 for Sai-Yang Zhang and No. 81673322 for Yan-Bing Zhang), China Postdoctoral Science Foundation (No. 2018M632812 for Sai-Yang Zhang), the Henan Scientific Innovation Talent Team, Department for Education (No. 19ITSTHN001 for Wen Zhao, China), Henan Association of Science and Technology (2020HYTP056) and Science and Technology Department of Henan Province (202102310144).

Appendix A. Supplementary data

Supplementary data to this article can be found online at https://doi.org/10.1016/j.ejmech.2020.112618.

References

[1] F. Bray, J. Ferlay, I. Soerjomataram, R.L. Siegel, L.A. Torre, A. Jemal, Global cancer statistics 2018: GLOBOCAN estimates of incidence and mortality worldwide for 36 cancers in 185 countries, Ca - Cancer J. Clin. 68 (2018) 394–424.

[2] M.-z. Qiu, R.-h. Xu, The progress of targeted therapy in advanced gastric cancer, Biomark. Res. 1 (2013) 32.

[3] W.W. Ma, A.A. Adjei, Novel agents on the horizon for cancer therapy, Ca - Cancer J. Clin. 59 (2009) 111–137.

[4] S. Jian, Q.-L. Gao, B.-W. Wu, D. Li, L. Shi, T. Zhu, J.-F. Lou, C.-Y. Jin, Y.-B. Zhang, S.-Y. Zhang, H.-M. Liu, Novel tertiary sulfonamide derivatives containing benzimidazole moiety as potent anti-gastric cancer agents: design, synthesis and SAR studies, Eur. J. Med. Chem. 183 (2019) 111731.

[5] M.A. Jordan, L. Wilson, Microtubules as a target for anticancer drugs, Nat. Rev. Canc. 4 (2004) 253–265.

[6] J.J. Field, A. Kanakkanthara, J.H. Miller, Microtubule-targeting agents are clinically successful due to both mitotic and interphase impairment of microtubule function, Bioorg. Med. Chem. 22 (2014) 5050–5059.

[7] A.E. Prota, K. Bargsten, D. Zurwerra, J.J. Field, J.F. Díaz, K.-H. Altmann, M.O. Steinmetz, Molecular mechanism of action of microtubule-stabilizing anticancer agents, Science 339 (2013) 587–590.

[8] Y. Lu, J. Chen, M. Xiao, W. Li, D.D. Miller, An overview of tubulin inhibitors that interact with the colchicine binding site, Pharm. Res. (N. Y.) 29 (2012) 2943–2971.

[9] A. Dorléans, B. Gigant, R.B. Ravelli, P. Mailliet, V. Mikol, M. Knossow, Variations in the colchicine-binding domain provide insight into the structural switch of tubulin, P. Nat. Acad. Sci. 106 (2009) 13775–13779.

[10] E.A. Perez, Microtubule inhibitors: differentiating tubulin-inhibiting agents based on mechanisms of action, clinical activity, and resistance, Mol. Canc. Therapeut. 8 (2009) 2086–2095.

[11] E.K. Rowinsky, R.C. Donehower, Paclitaxel (taxol), N. Engl. J. Med. 332 (1995) 1004–1014.

[12] S. Hill, S. Lonergan, J. Denekamp, D. Chaplin, Vinca alkaloids: anti-vascular effects in a murine tumour, Eur. J. Canc. 29 (1993) 1320–1324.

[13] A. Vacca, M. Iurlaro, D. Ribatti, M. Minischetti, B. Nico, R. Ria, A. Pellegrino, F. Dammacco, Antiangiogenesis is produced by nontoxic doses of vinblastine, Blood 94 (1999) 4143–4155.

[14] R. Kaur, G. Kaur, R.K. Gill, R. Soni, J. Bariwal, Recent developments in tubulin polymerization inhibitors: an overview, Eur. J. Med. Chem. 87 (2014) 89–124.

[15] L. Li, S. Jiang, X. Li, Y. Liu, J. Su, J. Chen, Recent advances in trimethoxyphenyl (TMP) based tubulin inhibitors targeting the colchicine binding site, Eur. J. Med. Chem. 151 (2018) 482–494.

[16] M. Kavallaris, Microtubules and resistance to tubulin-binding agents, Nat. Rev. Canc. 10 (2010) 194–204.

[17] B. Bumbaca, W. Li, Taxane resistance in castration-resistant prostate cancer: mechanisms and therapeutic strategies, Acta Pharm. Sin. B 8 (2018) 518–529.

[18] L. Li, S. Jiang, X. Li, Y. Liu, J. Su, J. Chen, Recent advances in trimethoxyphenyl (TMP) based tubulin inhibitors targeting the colchicine binding site, Eur. J. Med. Chem. 151 (2018) 482–494.

[19] Heterocyclic-fused pyrimidines as novel tubulin polymerization inhibitors targeting the colchicine binding site: structural basis and antitumor efficacy, J. Med. Chem. 61 (2018) 1704–1718.

[20] G. De Martino, M.C. Edler, G. La Regina, A. Coluccia, M.C. Barbera, D. Barrow, R.I. Nicholson, G. Chiosis, A. Brancale, E. Hamel, New arylthioindoles:? Potent inhibitors of tubulin polymerization. 2. Structure?Activity relationships and molecular modeling studies, J. Med. Chem. 49 (2006) 947–954.

[21] Z. Bai, M. Gao, H. Zhang, Q. Guan, J. Xu, Y. Li, H. Qi, Z. Li, D. Zuo, W. Zhang, BZML, a novel colchicine binding site inhibitor, overcomes multidrug resistance in A549/Taxol cells by inhibiting P-gp function and inducing mitotic catastrophe, Canc. Lett. 402 (2017) 81–92.

[22] M.T. Cui, L. Jiang, M. Goto, P.-L. Hsu, L. Li, Q. Zhang, L. Wei, S.-J. Yuan, E. Hamel, S.L. Morris-Natschke, In vivo and mechanistic studies on antitumor lead 7-Methoxy-4-(2-methylquinazolin-4-yl)-3,4-dihydroquinoxalin-2(1\r H\r)-one and its modification as a novel class of tubulin-binding tumor-vascular disrupting agents, J. Med. Chem. 60 (2017) 5586–5598.

[23] M.J. Pérez-Pérez, E.-M. Priego, O. Bueno, M.S. Martins, M.-D. Canela, S. Liekens, Blocking blood flow to solid tumors by destabilizing tubulin: an approach to targeting tumor growth, J. Med. Chem. 59 (2016) 8685–8711.

[24] R. Romagnoli, P.G. Baraldi, M.K. Salvador, F. Prencipe, C. Lopezcara, S.S. Ortega, A. Brancale, E. Hamel, I. Castagliuolo, S. Mitola, Design, synthesis, in vitro, and in vivo anticancer and antiangiogenic activity of novel 3-arylaminobenzofuran derivatives targeting the colchicine site on tubulin, J. Med. Chem. 58 (2015) 3209–3222.

[25] Laura Conesa-Milián, Eva Falomir, Juan Murga, Carda, Miguel, Meyen, Eef, Synthesis and biological evaluation of carbamates derived from amino-combretastatin A-4 as vascular disrupting agents, Eur. J. Med. Chem. 147 (2018) 183–193.

[26] N. Ty, G. Dupeyre, G.G. Chabot, J. Seguin, L. Quentin, A. Chiaroni, F.o. Tillequin, D. Scherman, S. Michel, X. Cachet, Structure–activity relationships of indole compounds derived from combretastatin A4: synthesis and biological screening of 5-phenylpyrrolo[3,4-a]carbazole-1,3-diones as potential anti-vascular agents, Eur. J. Med. Chem. 45 (2010) 3726–3739.

[27] P. Zhou, Y. Liang, H. Zhang, H. Jiang, Y. Wang, Design, synthesis, biological evaluation and cocrystal structures with tubulin of chiral β -lactam bridged combretastatin A-4 analogues as potent antitumor agents, Eur. J. Med. Chem. 144 (2017) 817–842.

[28] D.-Y. Oh, T.-M. Kim, S.-W. Han, D.-Y. Shin, Y.G. Lee, K.-W. Lee, J.H. Kim, T.-Y. Kim, I.-J. Jang, J.-S. Lee, Phase I study of CKD-516, a novel vascular disrupting agent, in patients with advanced solid tumors, Cancer. Rre. Treat. 48 (2016) 28–36.

[29] G.J. Rustin, G. Shreeves, P.D. Nathan, A. Gaya, T.S. Ganesan, D. Wang, J. Boxall, L. Poupard, D.J. Chaplin, M.R.L. Stratford, A Phase Ib trial of CA4P (combretastatin A-4 phosphate), carboplatin, and paclitaxel in patients with advanced cancer, Br. J. Canc. 102 (2010) 1355–1360.

[30] D.C. Blakey, F.R. Westwood, M. Walker, G.D. Hughes, A.J. Ryan, Antitumor activity of the novel vascular targeting agent ZD6126 in a panel of tumor models, Clin. Canc. Res. 8 (2002) 1974–1983.

[31] E. Fox, J.M. Maris, B.C. Widemann, W. Goodspeed, A. Goodwin, M. Kromplewski, M.E. Fouts, D. Medina, S.L. Cohn, A. Krivoshik, A phase I study of ABT-751, an orally bioavailable tubulin inhibitor, administered daily for 21 Days every 28 Days in pediatric patients with solid tumors, Clin. Canc. Res. 14 (2018) 1111–1115.

[32] C. Sessa, P. Lorusso, A. Tolcher, F. Farace, N. Lassau, A. Delmonte, A. Braghetti, R. Bahleda, P. Cohen, M. Hospitel, Phase I safety, pharmacokinetic and pharmacodynamic evaluation of the vascular disrupting agent ombrabulin (AVE8062) in patients with advanced solid tumors, Clin. Canc. Res. 19 (2013) 4832–4842.

[33] D.-J. Fu, P. Li, B.-W. Wu, X.-X. Cui, C.-B. Zhao, S.-Y. Zhang, Molecular diversity of trimethoxyphenyl-1, 2, 3-triazole hybrids as novel colchicine site tubulin polymerization inhibitors, Eur. J. Med. Chem. 165 (2019) 309–322.

[34] D.J. Fu, L. Fu, Y.-C. Liu, J.-W. Wang, Y.-Q. Wang, B.-K. Han, X.-R. Li, C. Zhang, F. Li, J. Song, Structure-activity relationship studies of β-Lactam-azide analogues as orally active antitumor agents targeting the tubulin colchicine site, Sci. Rep. 7 (2017) 12788.

[35] D.J. Fu, L. Ji-Feng, Z. Ruo-Han, L. Jia-Huan, Z. Sai-Yang, Z. Yan-Bing, Design and antiproliferative evaluation of novel sulfanilamide derivatives as potential tubulin polymerization inhibitors, Molecules 22 (2017) 1470.

[36] Md Ashraf, B. Thokhir, M. Shaik, Malik Shaheer, Syed Riyaz, Design and synthesis of cis-restricted benzimidazole and benzothiazole mimics of combretastatin A-4 as antimitotic agents with apoptosis inducing ability, Bioorg. Med. Chem. Lett 26 (2016) 4527–4535.

[37] A. Kamal, A. Mallareddy, M. Janaki Ramaiah, S.N.C.V.L. Pushpavalli, P. Suresh, C. Kishor, J.N.S.R.C. Murty, N.S. Rao, S. Ghosh, A. Addlagatta, Synthesis and biological evaluation of combretastatin-amidobenzothiazole conjugates as potential anticancer agents, Eur. J. Med. Chem. 56 (2012) 166–178.

[38] A.V. Subba Rao, K. Swapna, S.P. Shaik, V. Lakshma Nayak, T. Srinivasa Reddy, S. Sunkari, T.B. Shaik, C. Bagul, A. Kamal, Synthesis and biological evaluation of cis-restricted triazole/tetrazole mimics of combretastatin-benzothiazole hybrids as tubulin polymerization inhibitors and apoptosis inducers, Bioorg. Med. Chem. 25 (2017) 977–999.

[39] F.X. Yu, B. Zhao, K.L. Guan, Hippo pathway in organ size control, tissue homeostasis, and cancer, Cell 163 (2015) 811–828.

[40] R. Johnson, G. Halder, The two faces of Hippo: targeting the Hippo pathway for regenerative medicine and cancer treatment, Nat. Rev. Drug Discov. 13 (2014) 63–79.

[41] B. Zhao, K. Tumaneng, K.-L. Guan, The Hippo pathway in organ size control, tissue regeneration and stem cell self-renewal, Nat. Cell Biol. 13 (2011) 877–883.

[42] H.W. Park, K.-L. Guan, Regulation of the Hippo pathway and implications for anticancer drug development, Trends Pharmacol. Sci. 34 (2013) 581–589.

[43] T. Lu, Z. Li, Y. Yang, W. Ji, Y. Yu, X. Niu, Q. Zeng, W. Xia, S. Lu, The Hippo/YAP1 pathway interacts with FGFR1 signaling to maintain stemness in lung cancer, Canc. Lett. 423 (2018) 36–46.

[44] X. Wang, L. Su, Q. Ou, Yes-associated protein promotes tumour development in luminal epithelial derived breast cancer, Eur. J. Canc. 48 (2012) 1227–1234.

[45] S. Jiao, H. Wang, Z. Shi, A. Dong, Z. Zhou, A peptide mimicking VGLL4 function acts as a YAP antagonist therapy against gastric cancer, cancer, Cell 25 (2014) 166–180.

[46] Z.P. Xu, J.S. Zhu, Q. Zhang, X.Y. Wang, A breakdown of the Hippo pathway in gastric cancer, Hepato. Gastroenterol. 58 (2011) 1611.

[47] M. Santucci, T. Vignudelli, S. Ferrari, M. Mor, L. Scalvini, M.L. Bolognesi, E. Uliassi, M.P. Costi, The Hippo pathway and YAP/TAZ–TEAD protein–protein interaction as targets for regenerative medicine and cancer treatment, J. Med. Chem. 58 (2015) 4857–4873.

[48] S. Smith, R.B. Sessions, D.K. Shoemark, C.M. Williams, R. Ebrahimighaei, M.C. Mcneill, M.P. Crump, T.R. Mckay, G. Harris, A.C. Newby, Antiproliferative and antimigratory effects of a novel YAP–TEAD interaction inhibitor identified using in silico molecular docking, J. Med. Chem. 62 (2019) 1291–1305.

[49] D.-J. Fu, L. Zhang, J. Song, R.-W. Mao, R.-H. Zhao, Y.-C. Liu, Y.-H. Hou, J.-H. Li, J.-J. Yang, C.-Y. Jin, P. Li, X.-L. Zi, H.-M. Liu, S.-Y. Zhang, Y.-B. Zhang, Design and synthesis of formononetin-dithiocarbamate hybrids that inhibit growth and migration of PC-3 cells via MAPK/Wnt signaling pathways, Eur. J. Med. Chem. 127 (2017) 87–99.

[50] J. Song, X.-X. Cui, B.-W. Wu, D. Li, S.-H. Wang, L. Shi, T. Zhu, Y.-B. Zhang, S.-Y. Zhang, Discovery of 1,2,4-triazine-based derivatives as novel neddylation inhibitors and anticancer activity studies against gastric cancer MGC-803 cells, Bioorg, Med. Chem. Lett. 30 (2020) 126791.